PHILOSOPHICAL TRANSACTIONS OF THE ROYAL SOCIETY A MATHEMATICAL, PHYSICAL & ENGINEERING SCIENCES

Divergent-Beam X-Ray Photography of Crystals

Kathleen Lonsdale

Phil. Trans. R. Soc. Lond. A 1947 **240**, 219-250
doi: 10.1098/rsta.1947.0002

DIVERGENT-BEAM X-RAY PHOTOGRAPHY OF CRYSTALS

By KATHLEEN LONSDALE, F.R.S., *Royal Institution, London, W.*1

(*Received* 25 *June* 1945.—*Read* 21 *February* 1946)

[Plates 16 and 17]

Divergent-beam X-ray photography of single crystals by transmission can be used to study the 'extinction', that is, the diminution of the *transmitted* radiation that takes place at the Bragg reflexion angles. The intensity and geometry of the absorption lines observed give useful information about the texture of the crystal. Divergent beam photographs have shown that many crystals of organic compounds are unexpectedly perfect, and that sudden cooling to liquid-air temperatures will increase the mosaic character of their structure by an important factor and make them more suitable for structural analysis by the usual methods. Type I diamonds, and natural ice even near to its melting-point, are also found to possess a high degree of perfection, which cannot be removed by liquid-air treatment. The divergent beam method may be used for the determination of orientation, but it is important that the wave-length of X-rays employed should be correctly related to the size and nature of the crystal.

In certain favourable cases it is possible to make precision measurements of lattice constant or of wave-length from divergent beam photographs, without the use of any kind of precision apparatus. By such means it has been shown that the C—C distance in individual diamonds varies from 1541·53($\pm$0·02) to 1541·27*X*, (1·54465–1·54440 A), a difference presumably due to varying impurity content. Using diamond and a brass anticathode, the Zn $K\alpha_1$ wave-length, relative to Cu $K\alpha_1$ as 1537·40*X*, is found to be 1432·21($\pm$0·04) *X*. Temperature control would improve the accuracy of this measurement, which is, however, in good agreement with the latest value obtained by orthodox precision methods.

Introduction

W. H. Bragg (1914) was the first to observe, by means of the ionization spectrometer, that when a pencil of X-rays was selectively reflected from diamond, there was a diminution in the amount of radiation transmitted at the reflexion angle, an effect which he had expected, but which was not easily measurable.

In the same year, Rutherford & Andrade (1914) observed both reflexion and absorption lines photographically, using an effective point source of divergent γ-rays and a rock-salt crystal, and obtained thereby a measure of the wave-lengths of the monochromatic components of their radiation. This was the first application of divergent-beam crystal photography to such problems. Two years later H. Seemann (1916, 1917, 1919) developed an X-ray tube giving a wide-angle beam of Cu radiation and used it to obtain back-reflexion photographs from rock-salt. These showed a symmetrical pattern of reflexion conics when the crystal was placed with a symmetry axis normal to the photographic plate (Seemann 1930; Seemann & Kantorowicz 1930). Gerlach (1921 *a*, *b*) also developed a very simple tube giving a wide-angle beam of Cu radiation, and Hess (1937, 1942), using it, took transmission photographs of gypsum and mica. On these photographs, which were given an exposure of 90 min. with a crystal-to-plate distance of 1·64 cm., there was an intense inner disk showing no detail, together with a pattern of reflexion conics outside it.

Linnik (1929, 1930) used a fine pencil of X-rays, but rotated his crystal and photographic plate, rigidly fixed at a distance of 1·7 cm. apart, about a horizontal and a vertical axis,

shielding the plate from the direct X-ray beam by means of a screen, to prevent undue blackening of the background. He thus obtained a transmission photograph showing absorption conics and suggested that the same thing might be done more easily using a wide-angle beam, as, for example, a beam diverging from a pinhole, but that the inevitable background would spoil the pattern. He drew attention to the similarity between his transmission photographs and those of the Kikuchi line patterns obtained by electron diffraction methods (Kikuchi 1928 *a*, *b*). He also suggested that the method could be used for the determination of the positions of symmetry elements.

Fujiwara (1937, 1939) and Onoyama (1939), using a *convergent* primary X-ray beam, obtained black and white lines (reflexion and absorption conics) within the central shadow, which in the photographs taken by Hess had been too strongly exposed for observation of detail. The extent of the observed effect was necessarily restricted by the angle of the beam.

In all these cases the crystal was outside the X-ray tube. Kossel (1935, 1936 *a*, *b*, 1937) and his colleagues (Kossel & Voges 1935; Voges 1936) used a single crystal as anticathode *in* the X-ray tube, and generated divergent characteristic X-rays within the crystal itself; these were diffracted, according to the Bragg relation, from the various planes of the crystal before emergence, and a plane photographic plate placed some distance away from the aluminium window of the tube showed a pattern of black and white conics on a background of medium intensity. Borrmann (1935, 1936) also used the fluorescent rays from a single crystal as his divergent beam, but placed the crystal outside the tube and generated the radiation by means of an incident X-ray beam of higher frequency; he took back-reflexion photographs which showed both Laue spots (due to the incident pencil of high-frequency X-rays) and continuous reflexion conics (due to the divergent fluorescent low-frequency X-rays), and his exposures were of the order of 3 hr. Kossel (1936 *b*) used his method to obtain precision measurements of the lattice constant of copper, and van Bergen (1937, 1938, 1941) extended these measurements to calcite, NaCl, Al and α-Fe. Only the natural breadth of the X-ray emission lines set a limit to the accuracy of the experimental results, which was claimed to be of the order of 1 in 100,000.

A study of these experiments for a 'Report on X-ray Scattering in relation to Crystal Dynamics', then in preparation for the Physical Society of London (Lonsdale 1943), suggested to me that it would be of interest to extend experiments of this kind to the investigation of diamond and of crystals of carbon compounds. Dr A. Müller was kind enough to offer me the use of an X-ray tube he had designed which would give a beam of Cu radiation divergent externally through an angle of nearly 180°, and which was particularly well suited to my purpose. With this tube excellent photographs of the kind illustrated and described in this paper were obtained in exposure times varying from 3 sec. at a distance of 6 cm., using coarse-grained duplitized X-ray film, to 1 hr. or more using lantern slides (for finest resolution) at the same distance. Special process film (plate 17, figure 22 *d*) gives very clear and well-resolved pictures with an intermediate exposure. For a given photographic film, the time of exposure had a well-defined optimum, since under-exposure and over-exposure both spoilt the *contrast* between absorption lines and background which was aimed at in these experiments. Intensification was, of course, out of the question, since the spreading of the background thus produced would simply cause the complete disappearance of the absorption lines.

Simple geometrical theory

The X-rays diverge from a very small region (almost a point) on the exterior flat surface of the end of the tube; the crystal can therefore be mounted, in air, in contact with or very near to the X-ray source, and it is then irradiated by X-rays which meet the atomic planes at all angles. Laue (1935) has given a complete theory of the scattering of a divergent beam by a single crystal treated as a three-dimensional grating with extended base. A simpler and sufficiently accurate picture of the phenomenon is obtained by considering the Bragg reflexions from sets of parallel crystal planes of spacing d. It is clear that with a divergent beam, the X-rays of wave-length λ which satisfy the Bragg relation $\lambda = 2d\sin\theta$ will form the generators SA of a cone whose apex is at the source S and whose semi-vertical angle is $(\frac{1}{2}\pi - \theta)$ (figure 1). These X-rays, on reflexion in the direction AR, will be removed

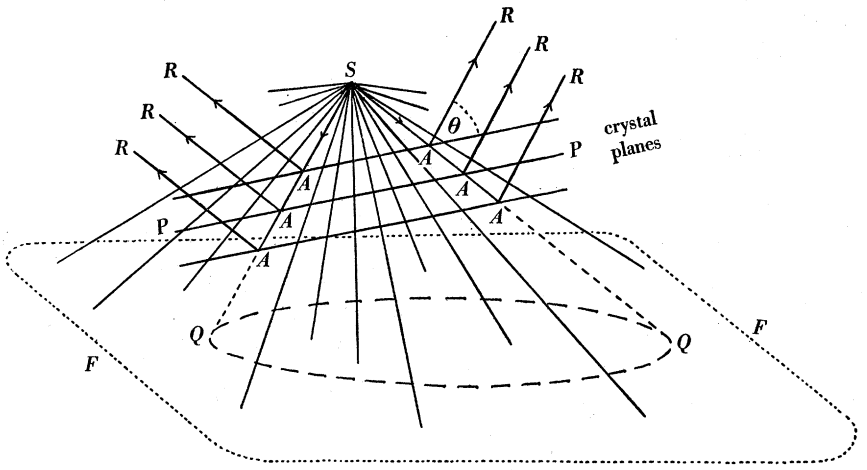

Figure 1. Removal of a cone of X-rays, by reflexion, from the general divergent beam. PP, reflecting crystal planes. QQ, absorption conic shown light against dark background. FF, photographic film.

from the general divergent beam, and there will, therefore, appear on the photographic plate or film FF an absorption conic QQ which will be *light* against a general darker background. This conic will be a circle only if the plane of the film is parallel to the reflecting planes PP. The directions AQ may be referred to as 'deficiency rays', since they are the directions in which rays are missing because of removal by reflexion. The deficiency rays, of course, represent a special case of absorption. In the case illustrated in figure 1, the reflected rays AR do not meet the photographic film at all; and it is generally true that the majority of lines recorded on such a transmission photograph will be absorption (deficiency) lines. If θ is not too large, however, and the reflecting planes (hkl) are inclined at a considerable angle to the plane film, the reflected rays may also be recorded on the photograph as a reflexion conic RR, which will be *darker* than the general background (figure 2). The set of planes $(\bar{h}\bar{k}\bar{l})$ will also give absorption and reflexion conics $Q'Q'$ and $R'R'$. Since in practice the planes (hkl) and $(\bar{h}\bar{k}\bar{l})$ will be separated only by a very small distance, the conics $R'R'$ and QQ (and similarly RR and $Q'Q'$) will be relatively close to each other. Before considering the

relative separation of black and white lines, however, and the properties of patterns given by symmetrical crystals, it is necessary to find out under what conditions these lines will be observable at all.

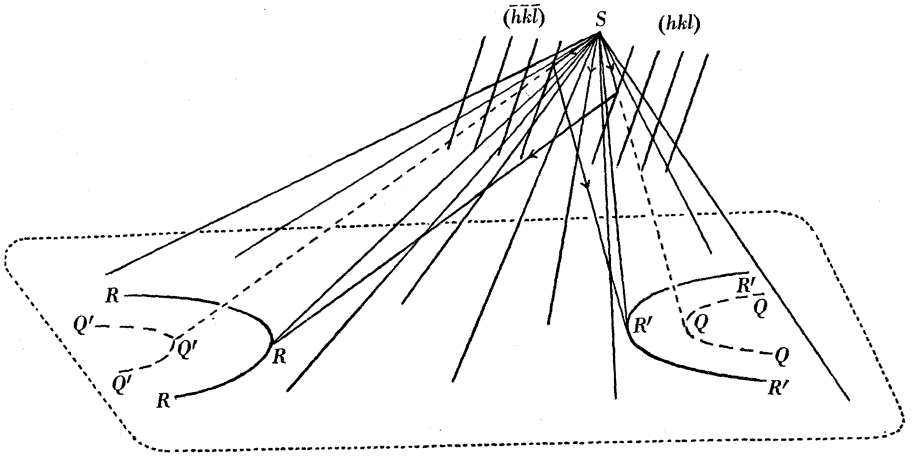

FIGURE 2. Formation of black and white conics by reflexion of rays from both sides of a set of planes.

RR, reflexion conic } corresponding to
QQ, deficiency conic } planes (*hkl*).

R'R', reflexion conic } corresponding to
Q'Q', deficiency conic } planes $(\bar{h}\bar{k}\bar{l})$.

Conditions under which no pattern is observed

In general, no absorption or reflexion lines will be observable (1) if the crystal is too nearly perfect; (2) if the crystal is too completely imperfect; (3) if the crystal is of unsuitable dimensions, either too small or too large, relative to the wave-length of X-rays used. The time of exposure must not, of course, lie outside certain limits, which are very dependent upon the kind of photographic plate or film used. This point has been mentioned in the Introduction.

(*a*) *Crystal perfection and extinction*

Andrade & Rutherford found that whereas a particular ordinary cleavage plate of rock-salt gave moderately good absorption lines, using a source of divergent γ-rays, crystals which were apparently much more perfect, as judged by specular reflexions of ordinary light, which were selected from a large number specially fetched from a salt mine, gave much inferior results.* Ewald & Renninger (1934; Renninger 1934) have shown that rock-salt crystals do vary in character from ideally mosaic to ideally perfect, according to their history of growth or mechanical deformation. They deduce that mosaic character is not determined by the *kind* of crystal considered, but is a property of the individual specimen, or of the large-scale crystallites that compose that specimen. A crystal may, for example, consist of a number of fairly large domains or crystallites whose angular displacement from an average orientation varies from 1 sec. to several degrees; yet each crystallite may be perfect in itself, so that the whole crystal shows the primary extinction characteristic of perfect crystals (Darwin 1914; Ewald 1918; James 1934). If the coherent domains (that is, regions in which there are no discontinuities of orientation or of spacing) are smaller, by an amount which depends upon the radiation used and the reflecting planes considered, primary extinction is reduced owing

* Private information kindly given to me by Professor E. N. da C. Andrade, F.R.S.

to the limitation of the interaction of the diffracted and transmitted rays, but secondary extinction, or partial shielding of the more distant by the nearer blocks, which also amounts to an effective increase in the coefficient of absorption at the reflecting angle, still occurs. When the size of the coherent domains is very small and the disorientation considerable, then both primary and secondary extinction are negligible and the crystal behaves as an ideal mosaic, the reflexions being several times as intense as for the perfect (whether monolithic or composite) specimen. A further reduction of block size results in a broadening of the reflexions (Bragg, Darwin & James 1926).

(*b*) *Perfect crystals*

When a perfect crystal is used, reflexion only takes place from the few crystal planes nearest to the source, and the angular range is only a few seconds (figure 3). The width of the deficiency ray is then decided by the width of the X-ray emission line itself and by the dimensions of the source *S*. If the specimen is a composite of largish perfect crystallites, the deficiency

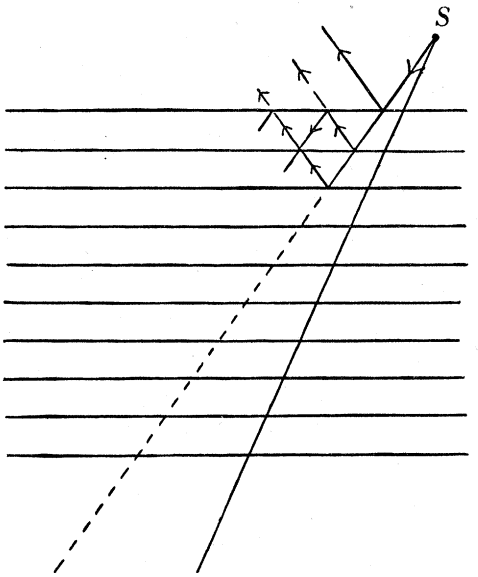

FIGURE 3. Reflexion and transmission by a perfect crystal.

ray may be composed of several individual fine rays, but its total (negative) intensity will be small, because the intensity of reflexion is small. Since the X-ray source is a very small region, approximating to a point, the deficiency and reflexion rays from a perfect crystal will give lines so fine and faint that they are either not visible or hardly show up at all against the background of general radiation. Photographs of this kind have been obtained from normal (type I) diamonds, calcite, rochelle salt, natural ice, and from some individual specimens of many organic compounds (plate 16, figure 20*a*).

(*c*) *Perfectly imperfect crystals*

The occurrence of deficiency rays is in general a demonstration of the existence of secondary extinction, that is, of an increase of absorption at the reflecting angle. If the crystal is so imperfect that all secondary extinction effects are smeared out, as, for example, in a block of crystallites of random or widely differing orientation (as in a finely divided

powder), then the average background absorption will be increased, but no discrete absorption lines will be observed at particular angles. This case is well illustrated by the use of diamond boart, carbonado or ballas.

(*d*) *Crystal size*

The intensity I of the X-rays transmitted through a thickness t of a given crystal is given by $I = I_0 e^{-\mu t}$, where I_0 is the incident intensity and μ the linear absorption coefficient for the given radiation. The longer the wave-length the greater the absorption, except in the neighbourhood of an absorption band. Care must, therefore, be taken that the absence of a picture is not due to absorption of practically *all* the characteristic radiation which is necessary to provide contrast, and the transmission only of short wave-length radiation. The crystal must be thick enough to build up a deficiency line of reasonable contrast, but not so thick that the characteristic *background* radiation is totally absorbed. The question of optimum thickness will be considered later.

Conditions under which a pattern is observed

(*a*) *Partly imperfect crystals*

Most single crystals are not perfect, nor are they ideally mosaic (James 1934). The planes of atoms of which they are composed are regular and parallel only over regions which are small compared with the size of the crystal itself. Two kinds of irregularities may be considered: there may be discontinuities without change of orientation, and there may be slight changes of orientation from one region or block to another. The theory of secondary extinction as usually applied in practice assumes that the latter kind of imperfection is the more important. In applying the formula $\mu' = \mu + gQ$, in which the normal absorption coefficient μ is increased at the reflecting angle by an amount proportional to the intensity of reflexion, all multiple reflexion by strictly parallel blocks within the crystal is ignored. Early experiments showed that in some cases (Bragg, James & Bosanquet 1921 *a*, *b*; James & Firth 1927) this was justified, but later investigation has indicated that a more rigorous formula of the type $\mu' = \mu + g_1 Q - g_2 Q^2 + \ldots$ (Darwin 1922) may sometimes be more appropriate. Thus it has been found (Brill, Grimm, Hermann & Peters 1939) that if the simple formula is used, then the apparent value of g obtained by comparing intensities of reflexion from a partly mosaic crystal of hexamine (hexamethylene tetramine) with those from a fine powder of that substance is much larger for planes having small Q values than for those of larger Q values. It is not constant. An expression of the type $\mu' = \mu + (g_1 - g_2 Q)\, Q$ would obviously fit such results better. It is clear that further experiment is required to test this point quantitatively. Unfortunately, secondary extinction is a quantity which it is difficult to measure with any degree of exactitude. An attempt to do so, by a successive approximation method, for one plane only of anthracene, was made by Robinson (1933), but he obtained results which were not only inconsistent when different wave-lengths were used, but which subsequent experiments with powdered anthracene (Robinson 1934) showed to have been of a wrong order of magnitude. [The value of g for the anthracene 002 reflexion deduced from Robinson's single-crystal experiments is 142. An approximate calculation based on a comparison of his more consistent experiments with anthracene powders gives $g > 600$.

Brill *et al.* (1939, p. 400), commenting on Robinson's method, say: '. . . alle *g*-Bestimmungen nach dieser Methode viel zu kleine Werte ergeben. In den von uns versuchten Fällen waren sie miest um etwa eine Zehnerpotenz zu klein.']

Now although the divergent beam method gives an excellent demonstration of the existence of secondary extinction, it cannot be used for its exact measurement. In the divergent beam method crystallites of slightly different orientations select the X-rays whose wave-lengths and directions suit them, and give one composite absorption line as a result. The accurate measurements of secondary extinction by a direct method would have to prevent this by the use of a monochromatic and strictly parallel beam. Nevertheless, the divergent-beam method can give much useful information about the texture of crystals.

(*b*) *Crystals of organic compounds*

It has generally been supposed that for crystals of organic compounds primary extinction is almost negligible and secondary extinction unimportant; that is, that they are almost ideally mosaic crystals. The fact that good divergent-beam photographs were obtained from a number of such crystals showed that this assumption was unsound, and that secondary extinction at least must be reckoned with, since it is by no means unimportant if it can give clear absorption lines. When later it was found that *some* crystals of organic compounds gave very poor divergent-beam photographs, it was difficult to decide *a priori* whether the absence of a picture in these cases was due to the presence of primary extinction (perfect crystal) or to the absence of secondary extinction (completely imperfect or mosaic crystal). Extended experiment showed that a wide variation existed. Three out of five crystals of oxalic acid dihydrate gave either no visible lines, or lines so faint as to be seen only with the greatest difficulty; the fourth gave a picture of moderate contrast and the fifth an excellent one. Very poor photographs were also given by erythritol, ammonium oxalate, stilbene, hexamethylenetetramine (plate 1, figure 20*a*), though all the crystals used were clear specimens with faces giving excellent optical reflexions. Sucrose, mannitol, tolane, *trans*azobenzene, 1.3.5-triphenylbenzene, penta-erythritol and penta-erythritol tetraphenyl ether gave lines of only moderate visibility. Anthracene, benzil, dibenzyl, benzophenone (plate 16, figure 20*c*), maleic acid, maleic anhydride, succinic acid, α-resorcinol, urea nitrate, hexamethylbenzene and hexaethylbenzene gave good, clear pictures, although even among these some were distinctly better than others. Only one or two crystals of each of these substances were examined, and the results should not necessarily be regarded as typical of the compounds in question.

Brill *et al.* (1939, p. 437) had found that by dipping a crystal of hexamethylenetetramine into liquid air they were able to produce a marked increase of reflecting power, that is, a marked decrease of perfection. Their crystal turned milky, showing that it had broken up into more of a mosaic. The same procedure was tried with two of the oxalic acid dihydrate crystals which had at first given poor divergent-beam photographs. They were dipped into liquid air for a few seconds and rephotographed when they had regained room temperature. The result was that a picture appeared where none had been seen previously. A second immersion improved the strength and visibility of the absorption lines. It was clear that these specimens had originally been so perfect as to exhibit considerable primary extinction. The sudden lowering of temperature to which they were subjected then broke down the

crystals into a partial mosaic and left only secondary extinction. The crystals became not only milky but very brittle. Presumably the small-scale breaking up of the structure into slightly disorientated crystallites (which, for complete absence of primary extinction, would have to be 1μ or less in linear dimensions) was accompanied by cracks on a much larger scale. Erythritol, stilbene and hexamethylenetetramine (plate 16, figures 20 *a*, *b*) also gave good pictures after immersion in, or spraying with, liquid air; and some of the specimens which had formerly given photographs of only moderate contrast (sucrose, mannitol and *trans*azobenzene were tested) gave much improved pictures after similar treatment. In all these cases there must have been considerable perfection to begin with. It is equally clear that secondary extinction remains even after drastic breaking down of the crystal perfection, and must be reckoned with for many reflexions, not merely the few most intense ones. Following the publication of a preliminary account of these experiments (Lonsdale 1944), it has become a routine practice in some X-ray crystal analysis laboratories to eliminate primary extinction by liquid-air treatment before structure investigation is begun.

(*c*) *Diamond*

It has been mentioned that type I diamonds (that is, diamonds showing groups of extra spots on Laue photographs) gave the bad divergent-beam photographs typical of perfect crystals. Only a few diamonds gave absolutely no picture at all (these photographs are not reproduced, since they show only background and no lines, whatever exposure time is used); these diamonds not only appeared to be perfect in form and optical properties, but showed the typical 'extra spots' (Lonsdale 1942 *a*, *b*) very strongly. It is difficult to reconcile these observations with the explanation of the extra spots given by Guinier (1942), who suggests that they are due to a partial irregularity of spacing in the cube directions. This explanation would account for many features of the extra spots satisfactorily; but why should this irregularity occur most markedly in the most perfect diamonds and not at all in mosaic specimens? Most type I diamonds gave pictures which showed very sharp lines, although with much less contrast (plate 16, figure 21 *b*) than the pictures given by type II diamonds (plate 16, figure 21 *a*). All type II diamonds gave excellent divergent-beam photographs, with high contrast. In some cases the lines were as sharp as those given by type I diamonds, but in others the lines were broadened, showing obvious distortion in certain directions (plate 17, figures 22 *a*, *b*, *c*). Nevertheless, in spite of this distortion, it is clear that strong secondary extinction persists. No amount of immersion in liquid air was able to change a type I into a type II diamond, or vice versa, or to affect their divergent-beam photographs in any way. Prolonged heat treatment in air, or at higher temperatures (up to 1250° C for 16 hr.) *in vacuo*, was equally ineffective.

Photometer measurements* have shown that the half-width at half-maximum of the diamond 331 Cu $K\alpha_1$ absorption line is $0{\cdot}25 \pm 0{\cdot}05$ of the α_1-α_2 separation. [The actual 331 Cu $K\alpha_1$-α_2 separation observed on photographs taken at 1 m. distance is 7 mm.] Compton & Allison (1935, p. 744) give the ratio of the natural half-width of the Cu $K\alpha_1$ emission line to the α_1-α_2 separation as 0·15. There is, therefore, some spreading of the diamond absorption lines, but this amounts to only about 2·4 min. of arc, and corresponds to a very small degree of disorientation of individual crystallites. It follows that the secondary extinction must result

* Made at the Cavendish Laboratory, Cambridge, with the kind help of Dr Lipson and Dr Wilson.

more from discontinuities of spacing between parallel crystallites than from lack of parallelism of the crystallites. One would expect to find, therefore, that multiple reflexion diminishes the extinction of the low-order as compared with the high-order reflexions. This is, indeed, the case, as may be seen from the following approximate calculations:

The actual intensity of the absorption line depends upon the amount of crystal traversed, but if measurements are made at comparable angles it is found that for an effective crystal thickness of 1·355 mm. the following relative intensities are recorded: (1) without the diamond in position (I_0), (2) with the diamond, but away from an absorption or reflexion line (I), (3) for the absorption lines 111 Cu $K\alpha_1$ (I_{111}); 220 Cu $K\alpha_1$ (I_{220}); 331 Cu $K\alpha_1$ (I_{331}); 331 Cu $K\alpha_2$ ($I_{331(2)}$);

$$I_0 : I : I_{111} : I_{220} : I_{331} : I_{331(2)} = 1270 : 368 : 335 : 343 : 346 : 356.$$

It is noteworthy that the absorption lines, although so clear, correspond to a reduction of the background intensity I by only 10–3 % or even less.

The relative intensities of the Cu $K\alpha_1$, Cu $K\alpha_2$, Cu $K\beta$ emission lines are about 10:5:2. It follows, therefore, that not more than 60 % of the emitted characteristic radiation can possibly be Cu $K\alpha_1$. Since the X-ray is run at a comparatively low voltage, for fear of piercing the window target, the percentage of white radiation emitted will be fairly high, but the exact amount and energy distribution is not known. For the purpose of our calculation we shall take as limits that the amount of Cu $K\alpha_1$ radiation emitted is, say, from 60 to 20 % of the total emitted radiation, represented by I_0. In terms of $I_0 = 1270$, it is seen that $762 > I_0^{\mathrm{Cu}\,K\alpha_1} > 254$. The intensity I after passing through thickness t of the diamond will depend on the effective linear absorption coefficient $\bar{\mu}$. Now μ is not known with certainty for diamond, even for a single wave-length. Values of μ/ρ varying from 5·5 to 3·84 have been recorded for carbon, using Cu $K\alpha$ radiation, but it is probable that all determinations using a powdered specimen are too high, owing to the unsuspected presence of secondary and perhaps even primary extinction. The value $\mu/\rho = 3{\cdot}84$ which was obtained by Brill *et al.* (1939, p. 418) using a diamond plate, is here accepted as a basis for approximate calculation. Since the density $\rho = 3{\cdot}515$ g./c.c., this gives $\mu = 13{\cdot}5$. If I_R is the intensity due to any emitted wave-length other than Cu $K\alpha_1$, and μ_R is the corresponding linear absorption coefficient, then I, the background intensity away from an absorption line, will be given by

$$I = \Sigma\Sigma\, I_R\, e^{-\mu_R t} + I_0^{\mathrm{Cu}\,K\alpha_1} e^{-13{\cdot}5t} = I_0\, e^{-\bar{\mu}t}$$

and I_{hkl}, the intensity at the absorption line due to the plane (hkl), will be

$$I_{hkl} = \Sigma\Sigma\, I_R\, e^{-\mu_R t} + I_0^{\mathrm{Cu}\,K\alpha_1} e^{-\mu' t},$$

where μ' is the linear absorption coefficient for Cu $K\alpha_1$ increased by secondary extinction. The difference

$$I - I_{hkl} = I_0^{\mathrm{Cu}\,K\alpha_1} (e^{-13{\cdot}5t} - e^{-\mu' t}),$$

and hence μ' may be found for various planes in terms of the relative values of I, I_{hkl}, $I_0^{\mathrm{Cu}\,K\alpha_1}$, t. Taking $I_0 = 1270$, $I - I_{111} = 33$, $I - I_{220} = 25$, $I - I_{331} = 22$, for $t = 0{\cdot}1355$ cm., and assuming $I_0^{\mathrm{Cu}\,K\alpha_1} < 762$, then $\mu'_{111} > 15{\cdot}9$, $\mu'_{220} > 15{\cdot}2$ and $\mu'_{331} > 15{\cdot}0$. According to the usual theory of secondary extinction, the difference between μ' and μ is dependent upon the intensity of reflecting power Q_{hkl}. Unfortunately, Q is also an uncertain quantity, the values given in

the literature varying among themselves over quite a wide range (Armstrong 1929; Brill *et al.* 1939, p. 430; Ponte 1927). Maximum and minimum estimates are as follows:

$$Q_{111}\ 0{\cdot}0768 \rightarrow 0{\cdot}0326, \quad Q_{220}\ 0{\cdot}0231 \rightarrow 0{\cdot}0163, \quad Q_{331}\ 0{\cdot}0153 \rightarrow 0{\cdot}0108,$$

and these, if substituted in the formula $\mu' = \mu + gQ$, give

$$g_{111}, 31 \rightarrow 74, \quad g_{220}, 74 \rightarrow 104, \quad g_{331}, 98 \rightarrow 139.$$

The values of g obtained by taking $I_0^{\mathrm{Cu}\,K\alpha_1} > 254$ are:

$$g_{111}, 159 \rightarrow 374, \quad g_{220}, 307 \rightarrow 436, \quad g_{331}, 373 \rightarrow 528.$$

Probably (owing to the divergency of the beam, as explained above) even these values are too low, but the special point to be noticed is that *g increases with decreasing Q*, and that the fact of this increase in independent of the particular values taken for $I_0^{\mathrm{Cu}\,K\alpha_1}/I_0$ or for Q_{hkl}. This confirms the hypothesis that in many type II diamonds the individual crystallites are closely parallel to each other, so that multiple reflexion is possible, although discontinuities at the boundaries interrupt the sequence of spacings and spoil the perfection of the crystal as a whole.

A few type II diamonds, however (plate 17, figure 22*c*) give photographs in which the 111 absorption lines although still sharp are outstandingly strong, while those corresponding to less intense reflexions are absent or very weak. This must mean that in these diamonds the secondary extinction is due mainly to the non-parallelism of the crystallites over a small range, and multiple reflexion is inconsiderable.

(*d*) *Thickness of specimen and time of exposure*

For any thickness t of the specimen $I = I_0\, e^{-\bar{\mu}t}$, where $\bar{\mu}$ is an effective value of the linear absorption coefficient for all wave-lengths present in various proportions in the primary beam. If the total intensity of the primary beam is K times that of the Cu $K\alpha_1$ component in it, then $I_0 = \mathrm{K} I_0^{\mathrm{Cu}\,K\alpha_1}$ and $I = \mathrm{K} I_0^{\mathrm{Cu}\,K\alpha_1} e^{-\bar{\mu}t}$. However, it is known that

$$I - I_{hkl} = I_0^{\mathrm{Cu}\,K\alpha_1}(e^{-\mu t} - e^{-\mu' t}),$$

and therefore

$$\frac{I - I_{hkl}}{I} = \frac{e^{-\mu t} - e^{-\mu' t}}{\mathrm{K} e^{-\bar{\mu}t}}.$$

The limiting value of $(I - I_{hkl})/I$, or the percentage weakening of the background in the region of an absorption line, is about 0·01 for visual observation.

For the particular diamond tested, $I/I_0 = 368/1270$ for $t = 0{\cdot}1355$ cm., and therefore $\bar{\mu} = 9{\cdot}16$. Since $\mu = 13{\cdot}5$ for Cu $K\alpha_1$ radiation, this shows that K must be large. Table 1 shows the results after taking the previous limits of value assumed for $I_0/I_0^{\mathrm{Cu}\,K\alpha_1}$.

TABLE 1. DIAMOND, Cu $K\alpha_1$

K = 1·67 (60 % Cu $K\alpha_1$); $\mu' = 15{\cdot}9$

t (cm.)	0·001	0·01	0·1	0·2	0·3	0·4	1·0
$\frac{e^{-13{\cdot}5t} - e^{-15{\cdot}9t}}{1{\cdot}67 e^{-9{\cdot}16t}}$	0·0014	0·0136	0·0822	0·0960	0·0834	0·0654	0·0072

K = 5 (20 % Cu $K\alpha_1$); $\mu' = 25{\cdot}7$

t (cm.)	0·001	0·01	0·1	0·2	0·3	0·4	1·0
$\frac{e^{-13{\cdot}5t} - e^{-25{\cdot}7t}}{5{\cdot}0 e^{-9{\cdot}16t}}$	0·0025	0·0220	0·0910	0·0764	0·0530	0·0352	0·0026

The optimum thickness of diamond for absorption-line contrast is therefore 1 *to* 2 *mm.*; the 111 line (which is the strongest) would probably not be visible at all if the diamond were $<0{\cdot}05$–$0{\cdot}1$ mm. or >7–9 mm. thick. The values of I corresponding to these two limiting thicknesses would be in the ratio of about 1000 to 1. Since the optimum time of exposure of a specimen 1 mm. thick is about 6 sec. at 6 cm., using duplitized blue-base X-ray film, the time of exposure corresponding to a specimen 0·08 mm. thick would be of the order of 0·1 sec., and that for a specimen 8 mm. thick would be of the order of 100 sec. [It is found that the time of exposure *v.* blackening curve is linear in the region of blackening required for visibility of absorption lines.] Similar thicknesses and times of exposure would be required for crystals of most organic compounds, using a Cu target.

Comparable figures for rock-salt (200 absorption line), with radiation from a Cu target, may be obtained by using the following experimental values (Bragg *et al.* 1921 *a*; James & Firth 1927) for g, Q_{200} and μ (NaCl, Cu $K\alpha$):

$$g = 320, \quad Q_{200} = 0{\cdot}1015, \quad \mu = 162, \quad \mu' = \mu + gQ = 194{\cdot}5.$$

The value of $\mu_{\lambda_1}/\mu_{\lambda_2}$ is approximately constant for Na and Cl within the range of wavelengths included in the primary beam, and therefore the effective linear coefficient for the primary beam, $\bar{\mu}$, may be taken as $9{\cdot}16/13{\cdot}5 \times 162$ or 110 approximately. Since g is now assumed, K can be omitted, the result being shown in table 2.

TABLE 2. NaCl, Cu $K\alpha_1$

t (cm.)	0·001	0·005	0·01	0·05	0·1
$\dfrac{e^{-162t} - e^{-194{\cdot}5t}}{e^{-110t}}$	0·0287	0·1097	0·1413	0·0352	0·0053

The optimum thickness of rock-salt for visibility of the 200 *absorption line using* Cu $K\alpha_1$ *radiation will be about* 0·05 *to* 0·1 *mm.*, therefore, and the lines will not be visible at all if the crystal is much less than 0·01 or greater than 0·5 mm. thick. In any case the contrast will be less for rock-salt than for diamond (when the factor K is inserted), using the same radiation and the optimum thickness of crystal in each case. It is clear that Cu radiation is unsuitable for the examination of crystals whose absorption coefficients are as high as, or higher than, that of NaCl.

If Mo $K\alpha$ radiation is used, the values $\bar{\mu} \sim 11{\cdot}2$, $\mu = 16{\cdot}53$, $\mu' = 23{\cdot}98$ (James & Firth 1927) are found for NaCl (200), as shown in table 3. The optimum thickness under these conditions will be 1 to 2 mm., and the limits of visibility will correspond approximately to $0{\cdot}05 < t < 6$ mm.

TABLE 3. NaCl, Mo $K\alpha$

t (cm.)	0·005	0·01	0·05	0·1	0·2	0·5	1·0
$\dfrac{e^{-16{\cdot}53t} - e^{-23{\cdot}98t}}{e^{-11{\cdot}2t}}$	0·0331	0·0681	0·2004	0·3089	0·2664	0·0676	0·0048

BLACK AND WHITE LINE WIDTH AND SEPARATION

In the case of a crystal which is of the correct order of thickness in relation to the wavelength employed, and which is sufficiently mosaic to give good secondary extinction but little primary extinction, planes will be reflecting throughout the whole thickness of the

crystal. One might expect, therefore, that although the absorption lines will be relatively narrow if the disorientation of individual crystallites is small, yet the reflexion lines should be broad (figure 4). In fact, the reflexion lines are usually little, if at all, broader than the absorption lines (plate 17, figure 22*c*). Rays reflected from planes near to the source, if they do not emerge at once from that side of the crystal, are lost by multiple reflexion and absorption. Only the rays reflected from planes in regions near to the surface (S' and S'' in figure 5)

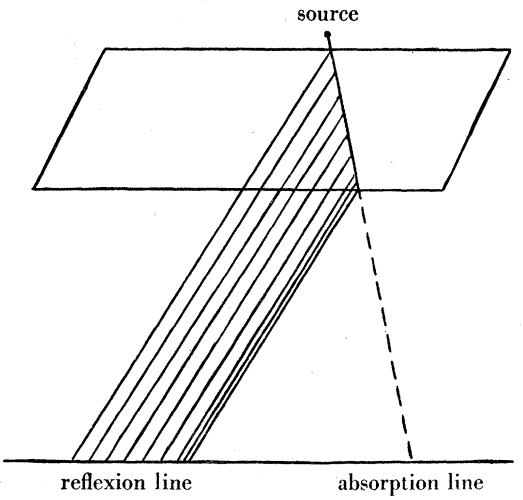

FIGURE 4. Reflexion and absorption in a crystal showing no multiple reflexion.

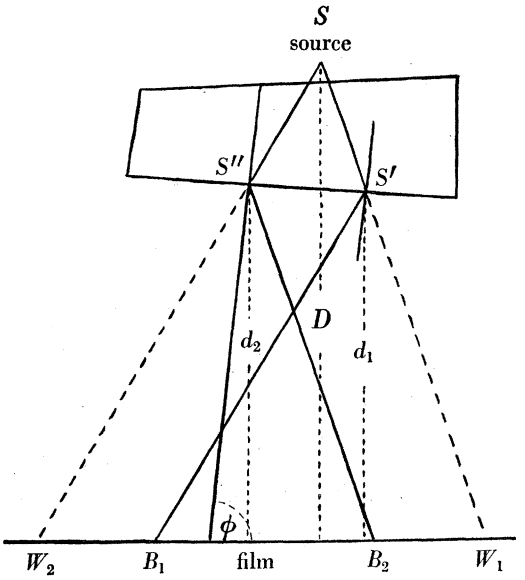

FIGURE 5

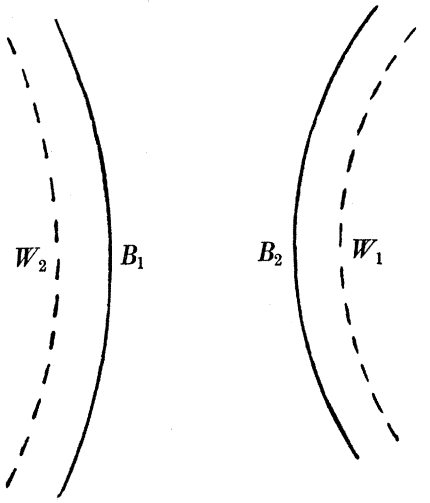

FIGURE 6

can emerge, to be recorded on the photographic film. Since, in the arrangement adopted, the film and the source of X-rays are on opposite sides of the crystal, the reflexion and deficiency rays will effectively come from opposite sides of the crystal (that is, from S', S'', and from the source S respectively). The reflexion and absorption conics corresponding to any one set of planes (hkl) will be sections of cones which are reflexions of each other, although the actual black and white curves traced on the film (B_1, W_1 in figure 6) will not necessarily be symmetrical in appearance. If the film is large enough to record both B_1 and W_1, however, it will also record the pair of conics B_2 and W_2 corresponding to the set of planes $(\bar{h}\bar{k}\bar{l})$. The conic

B_2 is parallel and close to the conic W_1 and similarly for B_1 and W_2. If D, d_1, d_2 are the perpendicular distances from S, S', S'' to the film, ϕ the acute angle between the reflecting planes and the plane of the film, and θ the glancing (Bragg) angle of reflexion, then the nearest distances of approach of the conics will be given by

$$W_1W_2 = D[\cot(\phi-\theta)-\cot(\phi+\theta)],$$
$$W_1B_1 = d_1[\cot(\phi-\theta)-\cot(\phi+\theta)],$$
$$W_2B_2 = d_2[\cot(\phi-\theta)-\cot(\phi+\theta)].$$

Hence
$$W_1B_2 = (D-d_2)[\cot(\phi-\theta)-\cot(\phi+\theta)] = \frac{(D-d_2)\sin 2\theta}{\sin^2\phi-\sin^2\theta},$$
$$W_2B_1 = (D-d_1)[\cot(\phi-\theta)-\cot(\phi+\theta)] = \frac{(D-d_1)\sin 2\theta}{\sin^2\phi-\sin^2\theta}.$$

The separation of the *parallel* black and white conics, therefore, is dependent on the distance from the X-ray source to the opposite side of the crystal, along a direction normal to the photographic film.

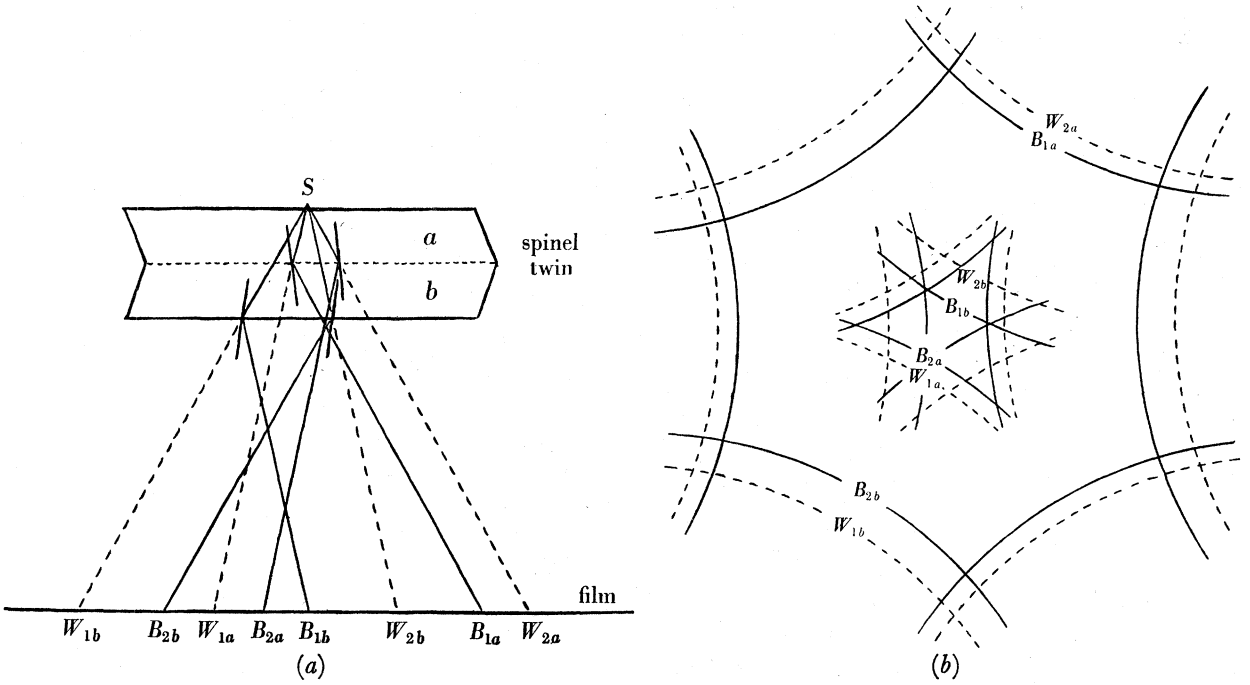

FIGURE 7. (*a*) Reflexion and absorption rays from spinel twin.
(*b*) Pattern of black and white lines observed.

If the crystal is a plate, placed parallel to the film, and the X-ray source is in contact with the crystal, $(D-d_1)$ or $(D-d_2)$ will be the actual thickness of the crystal plate. This dependence of the black-white line separation upon $(D-d)$ is well demonstrated either by moving the crystal farther from the source and noting the increasing separation, or by using a twin crystal. If, for example, a spinel twin of diamond is mounted with one individual in contact with the source (figure 7*a*), then the pattern obtained on a film placed normal to the common trigonal axis is as shown diagrammatically in figure 7*b*, the black-white line separation corresponding to one individual being approximately double that of the other, since the surface of one is twice as far from the X-ray source as that of the other.

When the crystals are badly distorted (plate 17, figure 22*b*) both black and white lines are broadened, but their mean distance apart is still given by the above relationship.

It is significant that on divergent-beam photographs of diamond showing marked distortion, the spreading of the high-order lines is certainly no larger than that of the low-order lines. *This proves that the line width is not due to a variation of spacing*, since a spacing variation is always much more marked for large values of the reflexion angles than for small values. The enhanced line width is probably due to a partial disorientation of quite large crystallites, each of which is composed of much smaller crystallites which are discontinuous but not disorientated relative to each other.

Geometry of patterns and methods of projection

Symmetrical patterns of considerable beauty are observed when crystals belonging to the higher classes of symmetry are photographed with axes or planes in positions having a simple geometrical relation to that of the photographic plate or film used (plate 17, figures 22*a*, 23*a*). In order to obtain the most complete pattern possible, a spherical camera would be required. This is not practicable, and a plane, or a semi-cylindrical film, is usually employed instead. Nevertheless, the geometry of the pattern to be expected from crystals of various symmetries is best considered in terms of a semi-spherical or spherical surface having the source of divergent radiation at its centre and the plane surface of the anti-cathode as a diametral plane. As examples, consideration in detail will be given later to the case of a cubic crystal (diamond) placed with a cube axis normal to the anti-cathode surface, and a hexagonal crystal (ice) placed with the hexagonal axis normal to that surface.

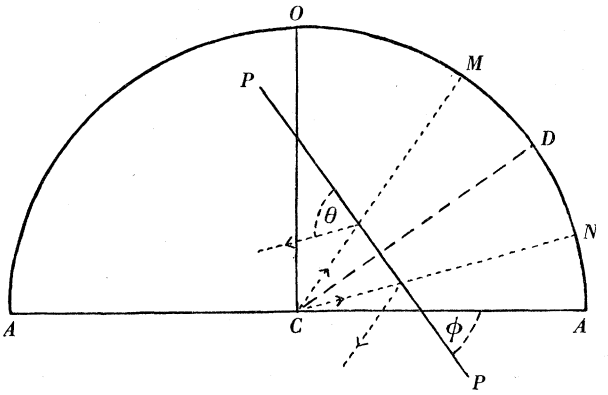

Figure 8. Production of absorption circle on sphere surrounding the crystal.

In general, let PP be any crystal plane making an angle ϕ with the diametral plane AA, and for which the Bragg angle is θ (figure 8). From C, the centre of the sphere, the normal to PP, (CD), meets the surrounding sphere of unit radius in D. CO is normal to AA, and therefore $\angle\, OCD = \phi$. The incident cone of rays from C which meet PP at the Bragg angle and are reflected away leaves an absorption cone meeting the sphere in a circle of diameter MN. The semi-vertical angle of the cone $(90° - \theta)$ is also the angular radius MCD of the circle MN; and $\angle\, DCA$, the altitude of CD, is $(90° - \phi)$. The projection of CD on to the diametral plane makes an azimuthal angle ω with some reference diameter RR. The three angles ω, ϕ, θ then define the position and size of the absorption circle of diameter MN. The positions of the

intersections of any such circles are easily determined by means of spherical triangles, and the whole pattern merely consists of a set of these intersecting circles.

In order to produce the pattern for purposes of reproduction, for study or for comparison with a photograph, four different methods could be used: (*a*) gnomonic, (*b*) orthogonal (Kossel), (*c*) cylindrical, (*d*) stereographic.

(*a*) *Gnomonic projection* is projection from the centre C on to a plane tangential at O and parallel to the diametral plane AA. If the angular distance, from O, of any point on the sphere is χ, then $\tan\chi$ will be the linear distance from O of the gnomonic projection of that point, since $CO = 1$. In general, the projection of any circle from the sphere on to the plane will be a conic section (figure 9).

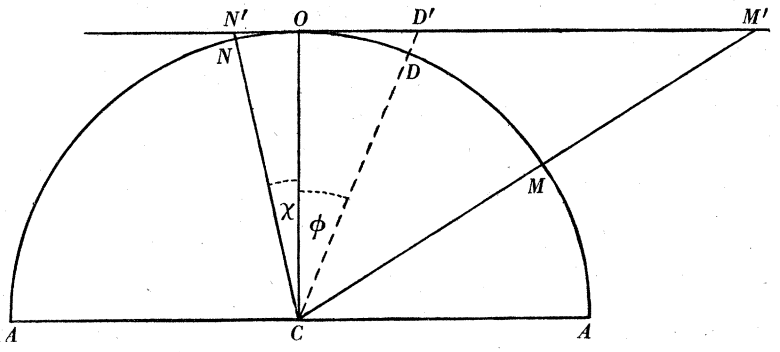

FIGURE 9. Gnomonic projection, N', D', M' are projections of N, D, M.

This gnomonic projection is useful in comparing the pattern found on a plane film placed parallel to the anticathode surface with the calculated pattern; but it is limited, in that only a very restricted amount of the spherical pattern can be projected on to a plane area of reasonable size (cf. plate 17, figure 22*a*).

(*b*) *Kossel projection.* Kossel and his colleagues have used an orthogonal projection of the spherical pattern on to the diametral plane AA. In this case the linear distance from C of any projected point is $\sin\chi$, and the projections of circles are no longer conic sections. This form of projection does show the whole pattern, but it is so crowded at the circumference as to be almost useless in that region (Renninger 1937 and figure 10). It does not correspond to any actual photograph that could be taken.

(*c*) *Cylindrical projection.* This can be used to compare the theoretical patterns with those that are actually observed on a film used in a semi-cylindrical camera and then straightened out. In a direction parallel to the axis of the cylinder linear distances are given by $\tan\chi$, in a direction normal to this by χ (cf. plate 17, figure 23*a*).

(*d*) *Stereographic projection.* The use of the stereographic projection for reproduction purposes was kindly suggested to me by Dr A. Müller and has proved most useful. It has the marked advantages that circles on the sphere appear as circles on the projection, and that the pattern is not too crowded at the circumference. It has the disadvantage that the projection of the centre of a circle is *not* the centre of the projected circle, and that therefore circles having common centres on the sphere (corresponding to absorption circles for the same plane in different orders, or using different wave-lengths of radiation) project into circles with different centres on the plane; in other words, circles or conics which are parallel on a photograph and which would be parallel on the sphere, are not parallel in the stereographic

projection. The radius of the projected circle is, as will be shown later, very dependent upon ϕ and, if θ is small, becomes exceedingly large as ϕ approaches 90°. Nevertheless, this method of representation is to be recommended as giving the most easily reproducible and understandable picture of the actual distribution of absorption rays in space.

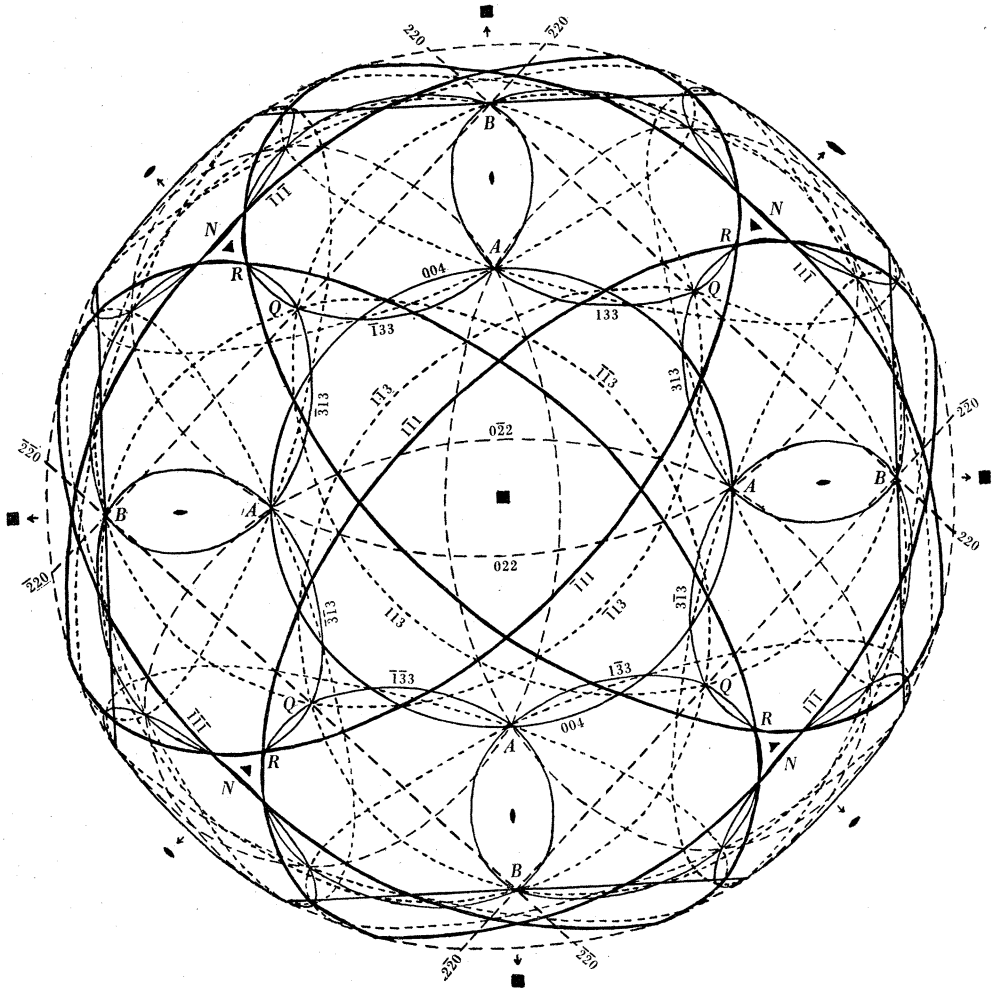

FIGURE 10. *Kossel projection.* Diamond, Cu $K\alpha_1$ radiation. Normal projection, on to a plane parallel to the cube face of the diamond, of the small circles in which absorption cones intersect a sphere surrounding the crystal: A and Q are points where several circles intersect.

In the stereographic projection, a point P at the lower extremity of the diameter OCP, normal to the diametral plane of the hemisphere, is the pole of projection. If lines are drawn from P to any point or curve on the surface of the upper hemisphere AOA, the point or curve in which these lines intersect the diametral plane AA is the stereographic projection. Figure 11 shows the construction by means of which it may be proved that circles MN on the sphere project into circles $M'N'$ on the plane, but that the centre of the projected circle is T', the projection of T (point of intersection of tangents from M, N and other points on small circle) and not D', the projection of D (the centre of the small circle). Then

$$\angle CPM' = \tfrac{1}{2}\angle OCM = \tfrac{1}{2}[\phi-(90^\circ-\theta)],$$
$$\angle CPN' = \tfrac{1}{2}\angle OCN = \tfrac{1}{2}[\phi+(90^\circ-\theta)].$$

If $CP = 1$, $\quad CM' = \tan \tfrac{1}{2}[\phi+\theta-90°], \quad CN' = \tan \tfrac{1}{2}[\phi-\theta+90°].$

Hence $$CT' = \tfrac{1}{2}[\tan \tfrac{1}{2}(\phi+\theta-90°) + \tan \tfrac{1}{2}(\phi-\theta+90°)],$$

$$M'T' = \tfrac{1}{2}[\tan \tfrac{1}{2}(\phi-\theta+90°) - \tan \tfrac{1}{2}(\phi+\theta-90°)].$$

These equations give the distance of the centre of the projected circle from the centre of the sphere, CT', and the radius of that circle, $M'T'$, in terms of ϕ and θ.

The stereographic projections of the diamond pattern found when a cube face of the diamond is parallel to the plane of projection are shown in figure 12, which is calculated for Cu $K\alpha_1$ radiation, and in figure 13, calculated for Zn $K\alpha_1$ radiation. The positions of the 4-, 3- and 2-fold axes of the crystal are quite clear.

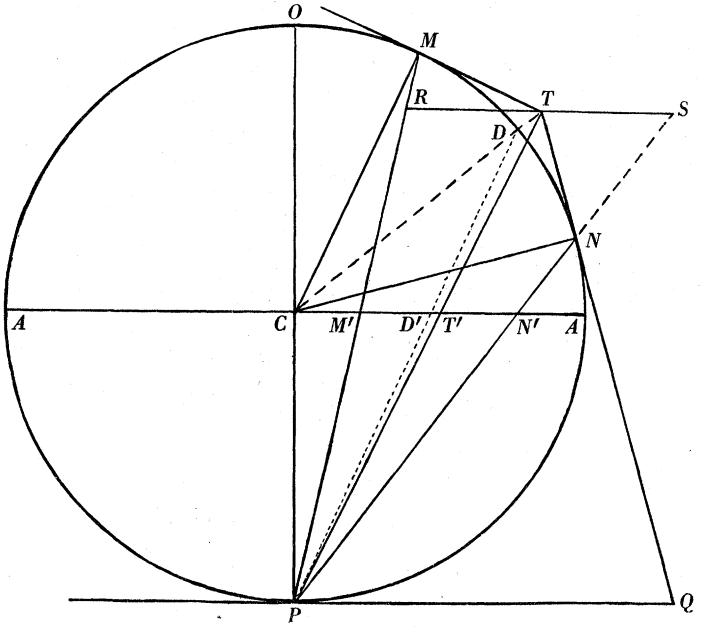

FIGURE 11. Stereographic projection, showing construction for proof that circle MN on sphere projects into circle $M'N'$ on diametral plane. P is pole of projection.

One feature of the patterns shown in figures 10 and 12, and in plate 17, figures 22*a* and 23*a*, is worthy of particular notice. There are certain points where more than two circles appear to intersect each other. These are shown enlarged in plate 16, figures 21 *c*, *d*. These same intersections occur in all the patterns, because a point of intersection on the surface of the sphere must be reproduced in any kind of projection. A special study of such intersections or 'coincidences' will be made in a later paragraph.

Plate 17, figure 23*b* shows a divergent-beam photograph of a diamond in which the cube face was not parallel to the surface of the anticathode. The pattern, however, is easily recognizable, and it may be seen that a (331) plane is nearly parallel to the film. The exact positions of the symmetry axes are easily located, and it is a matter of simple geometry to determine the crystal orientation when this is unknown.

All cubic crystals will, of course, give very similar patterns, although certain lines will be present in some and absent in others, and the scale of the pattern will change. Plate 17, figure 22*a* shows the pattern given by diamond when an octahedral plane is parallel to the

surface of the anticathode and to the (plane) film, and it is instructive to compare this with the pattern given by a copper single crystal, as published by Voges (1936).

Patterns given by hexagonal crystals will vary more, since there are two lattice constants instead of one only. Figure 14 shows the stereographic projection of the pattern given by ice, using Cu $K\alpha_1$ radiation, when the principal plane (0001) is parallel to the face of the anticathode and to the plane film. Only observed absorption lines are shown in the diagram,

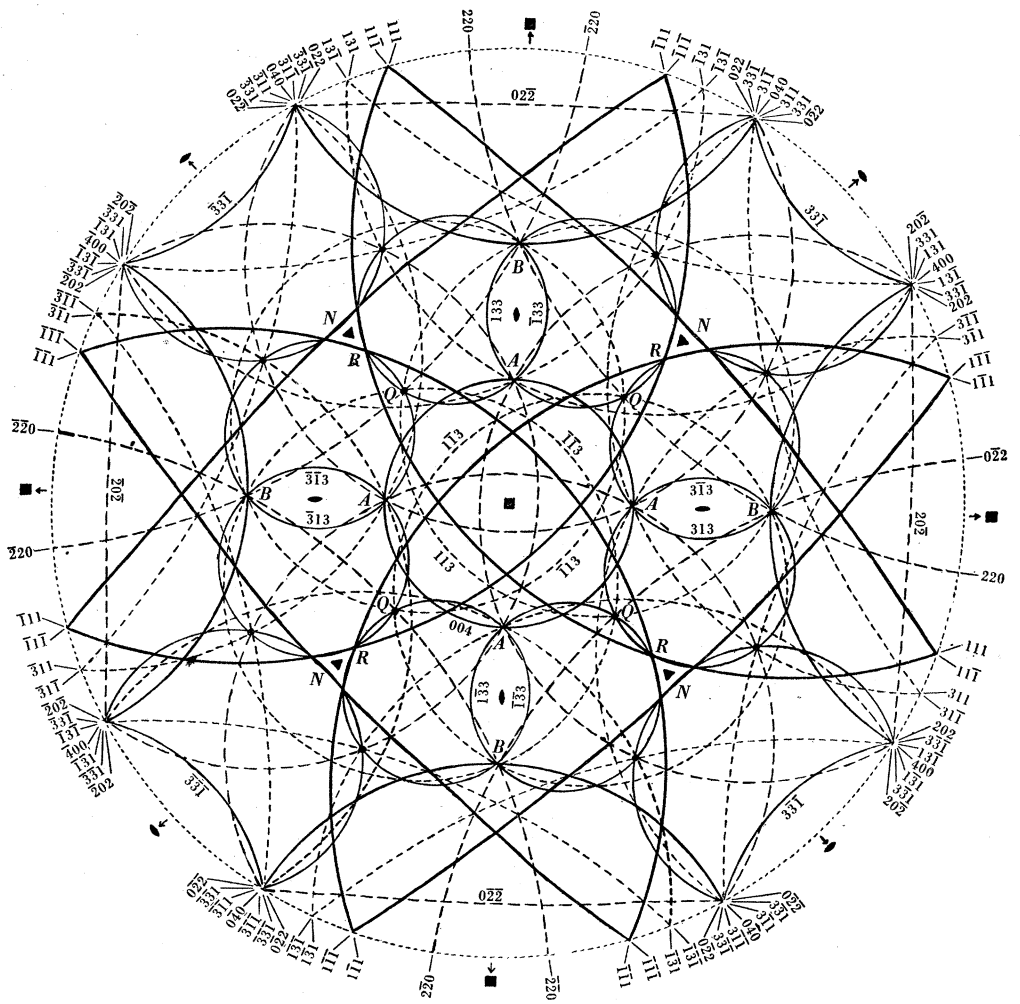

FIGURE 12. *Stereographic projection.* Diamond, Cu $K\alpha_1$ radiation, on plane parallel to cube face of crystal, showing coincidences of several circles at A and Q. This projection may be compared with the photograph shown in plate 17, figure 23*a*, which was taken on a semi-cylindrical film, remembering, however, that the photograph shows lines corresponding to Cu $K\alpha_1$, α_2 and β radiations.

which may be compared with plate 16, figure 20*d*. Contrary to expectation, the lines obtained from a single crystal of natural ice (grown on the surface of water in a basin, during cold weather) were extremely fine and sharp when they could be seen at all, and it was often found that no pattern, or only the faintest pattern, appeared even when the ice crystal used was of suitable thickness and gave a good Laue photograph. This seems to indicate a high degree of perfection in natural ice crystals even near to 0° C, an indication which is confirmed by the fact that reflexions from as many as seven planes did show secondary extinction in

some, presumably more mosaic, specimens, and by the further observation that, on the whole, the single ice crystals were rather weak reflectors when the usual parallel-beam methods were used.

It will be noticed that the lines in divergent-beam photographs of ice and also in those of less symmetrical organic compounds, are much less *curved* than many of those in diamond photographs (cf. plate 16, figures 20 *c*, *d* and plate 17, figure 23 *b*, *c*). This is because diamond

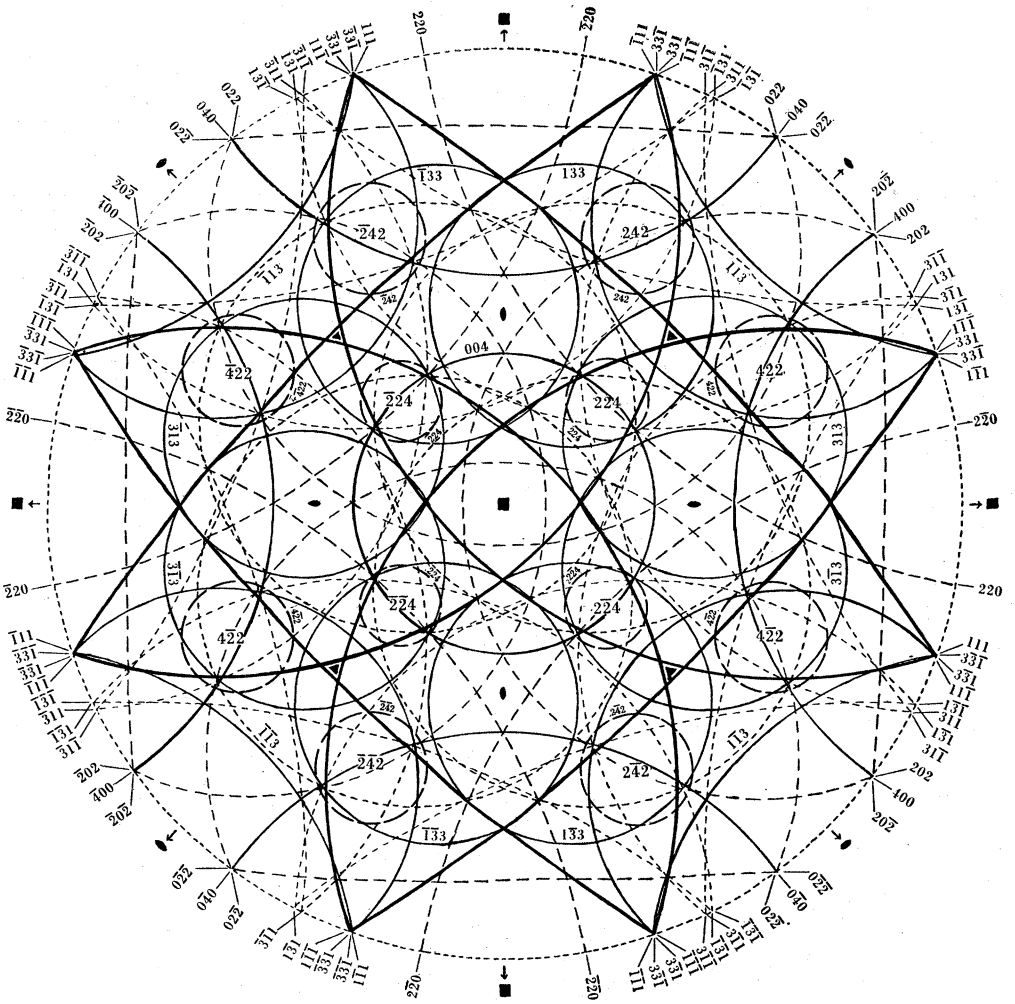

FIGURE 13. *Stereographic projection.* Diamond, Zn $K\alpha_1$ radiation, on plane parallel to cube face of crystal, showing small circles due to {224} high-angle reflexions, not observable when Cu $K\alpha$ radiation is used, but observed with Cu $K\beta$ radiation (cf. plate 17, figures 23 *c* and 22 *d*).

has relatively strong reflexions for which the Bragg angle is large, and for which, therefore, the semi-vertical angles $(90° - \theta)$ of the secondary extinction cones are small. Owing to the sharp falling off of the atomic scattering factors of carbon, oxygen, etc., in organic crystals, there are usually no high-angle reflexions of observable intensity. An exception occurs for hexamethylbenzene, which does show some absorption lines of marked curvature, corresponding to high-angle reflexions of unusual intensity (Lonsdale 1929). In the case of ice there *are* high-angle reflexions, but they are not intense enough to show secondary extinction.

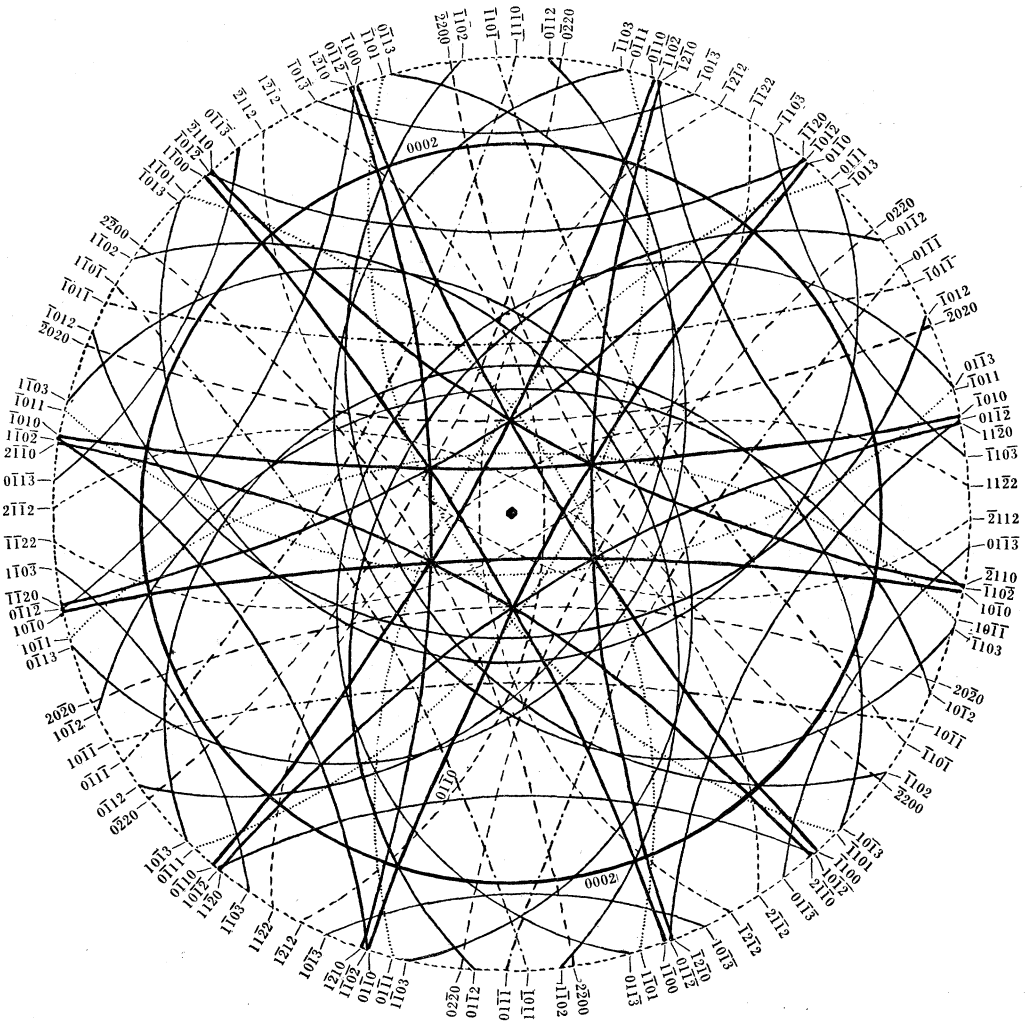

FIGURE 14. *Stereographic projection.* Natural ice near 0° C. Cu $K\alpha_1$ radiation; (0001) plane parallel to plane of projection. Only observed lines are shown. (In diamond all possible lines were observed.)

CONDITIONS FOR GEOMETRICAL OR ACCIDENTAL COINCIDENCE OF LINE INTERSECTIONS

For crystals of high symmetry there are, as mentioned previously, a number of points in the total pattern at which several absorption lines intersect. In order to study where these may occur it is simplest to consider the special case of diamond, and spherical trigonometry will be used to locate the intersections of small circles of given size and position on the surface of a sphere.

The point A (figure 10 or 12) is the intersection of the $0\bar{2}2$, 022 circles and also apparently of the 004, $3\bar{1}1$, 311, $3\bar{1}3$, 313 circles. Let us see which of these coincidences is geometrically inevitable for all wave-lengths, and which takes place only for Cu $K\alpha_1$ radiation; also if, in the latter case, it is exact. The values of ω, relative to the [100] direction; ϕ, relative to the [001] direction; and θ, which determine the centres and radii of these circles on a sphere of unit radius, are given in table 4.

TABLE 4

hkl	ω	ϕ	θ
004	—	0	$\sin^{-1} 2\frac{\lambda}{a}$
022	90°	45°	$\sin^{-1} \sqrt{2}\frac{\lambda}{a}$
$0\bar{2}2$	−90°	45°	$\sin^{-1} \sqrt{2}\frac{\lambda}{a}$
311	$\tan^{-1} \frac{1}{3}$	$\tan^{-1} \sqrt{10}$	$\sin^{-1} \frac{\sqrt{11}}{2}\frac{\lambda}{a}$
$3\bar{1}1$	$-\tan^{-1} \frac{1}{3}$	$\tan^{-1} \sqrt{10}$	$\sin^{-1} \frac{\sqrt{11}}{2}\frac{\lambda}{a}$
313	$\tan^{-1} \frac{1}{3}$	$\tan^{-1} \sqrt{10/3}$	$\sin^{-1} \frac{\sqrt{19}}{2}\frac{\lambda}{a}$
$3\bar{1}3$	$-\tan^{-1} \frac{1}{3}$	$\tan^{-1} \sqrt{10/3}$	$\sin^{-1} \frac{\sqrt{19}}{2}\frac{\lambda}{a}$

For 004, the angular distance OA (that is, the angular distance from O, the point of emergence of the cube axis [001] to the circumference of the extinction circle) is $90^\circ - \theta_{004}$, or $\cos^{-1} 2\frac{\lambda}{a}$. The angular distance OA', where A' is the point of intersection of circles 022 and $0\bar{2}2$, is found by solving the spherical triangle DOA', D being the centre of the circle 022 (figure 15):

$$DA' = 90^\circ - \theta_{022} = \cos^{-1} \sqrt{2}\frac{\lambda}{a}, \quad OD = \phi_{022} = 45^\circ, \quad \angle DOA' = 90^\circ.$$

Hence

$$OA' = \cos^{-1} [\cos (90^\circ - \theta_{022})/\cos \phi_{022}]$$
$$= \cos^{-1} [\sqrt{2} \sin \theta_{022}] = \cos^{-1} 2\frac{\lambda}{a} = OA.$$

It follows that 022 and $0\bar{2}2$ intersect each other at a point on the 004 circle for any wavelength and any cubic lattice constant. This can be checked on plate 16, figure 21*c*, which shows the Cu $K\alpha_1$ and α_2 intersections, and on figures 12 and 13 for Cu $K\alpha_1$ and Zn $K\alpha_1$.

The intersection of 311, $3\bar{1}1$ necessarily occurs along the *direction* OA, for which $\omega = 0$, but not necessarily at A. First consider the triangle ODT (figure 16), where T is the midpoint between the centres of 311 and $3\bar{1}1$.

$$\angle DTO = 90^\circ, \quad \angle DOT = \tan^{-1} \tfrac{1}{3}, \quad DO = \phi = \tan^{-1} \sqrt{10}.$$

Therefore

$$OT = \tan^{-1} [\cos (\tan^{-1} \tfrac{1}{3}) \tan \phi] = \tan^{-1} 3,$$

and

$$TD = \cos^{-1} [\cos \phi/\cos (\tan^{-1} 3)] = \cos^{-1} \sqrt{\tfrac{10}{11}}.$$

Now in the right-angled spherical triangle $A''TD$,

$$\angle A''TD = 90^\circ, \quad TD = \cos^{-1} \sqrt{\tfrac{10}{11}}, \quad DA'' = 90^\circ - \theta_{311}.$$

Hence

$$A''T = \cos^{-1} [\cos (90^\circ - \theta_{311})/\sqrt{\tfrac{10}{11}}]$$
$$= \cos^{-1} [\sqrt{\tfrac{11}{10}} \sin \theta_{311}] = \cos^{-1} \frac{11}{2\sqrt{10}}\frac{\lambda}{a},$$

$$OA'' = \tan^{-1} 3 - \cos^{-1} \frac{11}{2\sqrt{10}}\frac{\lambda}{a}.$$

Now there is, from this formula, no geometrical reason why A'' should coincide with A, and in fact it only appears to do so for one particular wave-length value, that of Cu $K\alpha_1$. The photographs (plate 16, figure 21 *c*, and others not reproduced) and the figures 12 and 13 show that the intersection of 311, $3\bar{1}1$ is only coincident with that of 004, 022 and $0\bar{2}2$ for Cu $K\alpha_1$ radiation, and not for Cu $K\alpha_2$, Cu $K\beta$ or Zn $K\alpha$.

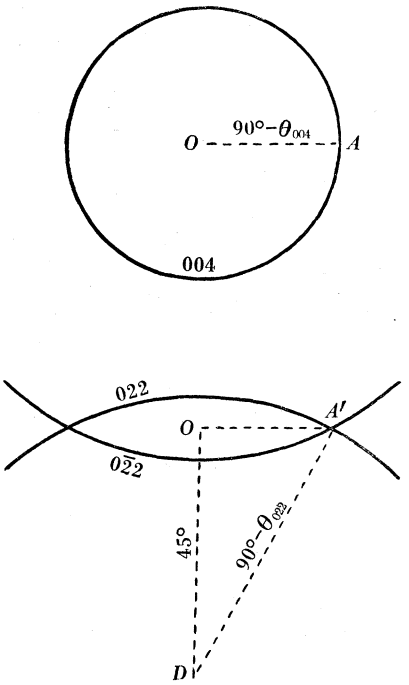

FIGURE 15

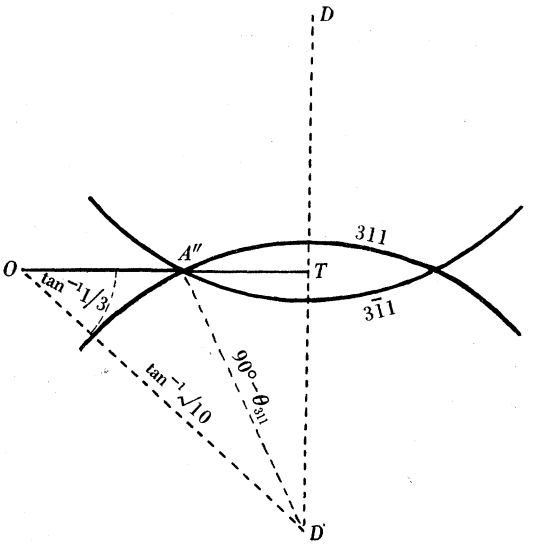

FIGURE 16

The same is true of the intersection of the 313, $3\bar{1}3$ circles, which occurs at a point A''' along the direction OA, but at an angular distance from O given by

$$OA''' = 45° - \cos^{-1}\frac{19}{6\sqrt{2}}\frac{\lambda}{a}.$$

Spacing or lattice constant measurement

Since A, A'' and A''' do, in fact, coincide for a particular and accurately known value of λ, a precision determination of the lattice constant a can be made by solving the equations

$$\cos^{-1}2\frac{\lambda}{a} = \tan^{-1}3 - \cos^{-1}\frac{11}{2\sqrt{10}}\frac{\lambda}{a} = \tan^{-1}1 - \cos^{-1}\frac{19}{6\sqrt{2}}\frac{\lambda}{a}.$$

This may be done graphically (knowing a approximately), and it is found that for $\lambda = 1537{\cdot}400X$ (Wennerlöf 1930; Bearden & Shaw 1935), the equations are satisfied when $a = 3559{\cdot}7X$; but the variation of OA''' or of OA'' with small changes in λ/a is not so marked that it is possible to determine a to a greater degree of accuracy than is given by the first place of decimals of X units.

The points A are not, however, the only points from which an estimate of the lattice constant may be made. The distances of A and other important points on the absorption circles from the cube axis CO, all in terms of angular distances on the hemisphere, are given in table 5.

TABLE 5

circles involved	description of point	distance	direction ω
004	any point A on circle	$OA = \cos^{-1} 2\frac{\lambda}{a}$	0°
400	nearest point B to O	$OB = \sin^{-1} 2\frac{\lambda}{a}$	0°
022, $0\bar{2}2$	intersection A	$OA = \cos^{-1} 2\frac{\lambda}{a}$	0°
220	nearest point Q to O	$OQ = \sin^{-1} \sqrt{2}\frac{\lambda}{a}$	45°
$11\bar{1}$	nearest point N to O	$ON = 90° - \tan^{-1}\sqrt{2} + \sin^{-1}\frac{\sqrt{3}}{2}\frac{\lambda}{a}$	45°
$\bar{1}11$, $1\bar{1}1$	intersection R	$OR = \cos^{-1}\frac{3}{2}\frac{\lambda}{a}$	45°
311, $3\bar{1}1$	intersection A''	$OA'' = \tan^{-1} 3 - \cos^{-1}\frac{11}{2\sqrt{10}}\frac{\lambda}{a}$	0°
$\bar{1}13$, $1\bar{1}3$	intersection Q'	$OQ' = \cos^{-1}\frac{11}{6}\frac{\lambda}{a}$	45°
331	nearest point N' to O	$ON' = \tan^{-1} 3\sqrt{2} - 90° + \sin^{-1}\frac{19}{2}\frac{\lambda}{a}$	45°
313, $3\bar{1}3$	intersections A''', B'''	$\begin{matrix} OA''' \\ OB''' \end{matrix} = 45° \mp \cos^{-1}\frac{19}{6\sqrt{2}}\frac{\lambda}{a}$	0°
313, 133	intersections Q'', R'	$\begin{matrix} OQ'' \\ OR' \end{matrix} = \tan^{-1}\frac{2\sqrt{2}}{3} \mp \cos^{-1}\frac{19}{2\sqrt{17}}\frac{\lambda}{a}$	45°
224	farthest point R'' from O	$OR'' = 90° + \tan^{-1}\sqrt{5} - \sin^{-1}\sqrt{6}\frac{\lambda}{a}$	45°
422, 242	intersections V, W	$\begin{matrix} OV \\ OW \end{matrix} = \tan^{-1}\frac{3}{\sqrt{2}} \mp \cos^{-1} 6\sqrt{\frac{2}{11}}\frac{\lambda}{a}$	45°

Several of these points will give an accurate value of a. For instance, it may be seen on the photograph shown in plate 17, figure 22 *d*, that the 331 Cu $K\alpha_1$ and α_2 lines *bracket* the $11\bar{1}$ line in the neighbourhood of the point N. The inequality

$$\left[\tan^{-1} 3\sqrt{2} + \sin^{-1}\frac{19}{2}\frac{\lambda}{a} - 90°\right]_{\text{Cu } K\alpha_2} > \left[90° - \tan^{-1}\sqrt{2} + \sin^{-1}\frac{\sqrt{3}}{2}\frac{\lambda}{a}\right]_{\text{Cu } K\alpha_1} > \left[\tan^{-1} 3\sqrt{2} + \sin^{-1}\frac{19}{2}\frac{\lambda}{a} - 90°\right]_{\text{Cu } K\alpha_1},$$

can also be used to give a value of a accurate to the first place of decimals of X units.

The most accurate estimate of a, however, is given by a consideration of the points Q, where there is a near coincidence of lines 220, $\bar{1}13$, $1\bar{1}3$, 313 and 133, and where the last two circles intersect so obliquely that a small change in λ/a would produce a large movement of the point of intersection Q''. On the actual photographs used for measurement (cf. plate 16, figure 21 *d*), which were enlargements $\times 2$ of films placed at 1 m. distance from the X-ray source and crystal, the change of λ from 1541·231X (Cu $K\alpha_2$) to 1537·400X (Cu $K\alpha_1$) causes a shift of about 6·2 cm. in the position of Q''. In other words the value of

$$\left[\tan^{-1}\frac{2\sqrt{2}}{3} - \cos^{-1}\frac{19}{2\sqrt{17}}\frac{\lambda}{a}\right]$$

changes very rapidly as λ/a varies (figure 17). The positions of the 220 Cu $K\alpha_1$ and α_2 lines, and therefore of Q for each of these lines, do not change at all rapidly, because $\sin^{-1}\sqrt{2}\,(\lambda/a)$ is not at all sensitive to a change in λ/a. The relative position of the 313, 133 Cu $K\alpha_1$ intersection, with reference to the 220 Cu $K\alpha_1$ and α_2 lines (see plate 16, figure 21 *d*, and inset to figure 17) is a most sensitive indicator of the exact value of λ/a, or since λ is accurately known, of a in terms of λ as a standard. Each mm. variation in the relative position of the line intersection Q'' on the enlarged photographic print corresponds to a change in a of about 1 in 20,000 or of 0·18X.

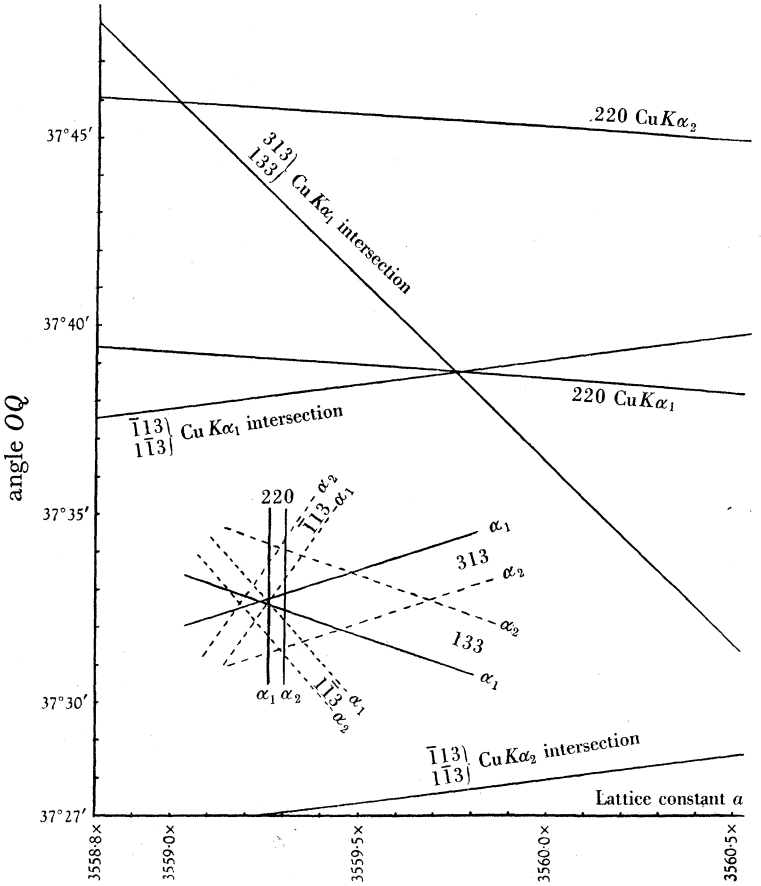

FIGURE 17. Measurement of diamond lattice constant from position of 313, 133 Cu $K\alpha_1$ intersection relative to the 220 Cu $K\alpha_1$ and α_2 lines. Abscissae give lattice constant of diamond, uncorrected for temperature, but using wave-lengths corrected for refractive index. Ordinates give angles OQ measured from direction of cube axis. 4 mm. on photographic print approx. equals 7 min. of arc.

The obvious advantage of a method such as this, which depends only on the position of a point relative to two lines in its very close neighbourhood, is that no precision apparatus is required. In fact, the film was held in a light-tight envelope, by a retort stand placed at about 1 m. from the crystal. The exactness of the distance does not matter, nor does the exact orientation of the film relative to the crystal axes and anticathode surface, as long as the 220 Cu $K\alpha_1$ and α_2 lines are well resolved. Their actual separation on the photograph before enlargement was 2 mm. and the apparent (visual) width of each line about 0·5 mm.

It will be clear that since we are now concerned with the second place of decimals of X units, the refractive index of the diamond for Cu K radiation must be taken into account.

The wave-length λ_0 of Cu $K\alpha_1$ radiation, *in vacuo* (or air) is $1537{\cdot}400X$. In a crystal the wave-length is effectively increased, to λ, by about $0{\cdot}00112\,\%$ in the case of diamond

$$[\mu = \lambda_0/\lambda = 1 - 1{\cdot}35\rho\lambda_0^2 \times 10^{10}, \quad \text{where } \rho \text{ is the crystal density}].$$

The Bragg relation, $n\lambda = 2d\sin\theta$, applies *within the crystal*, but θ cannot be measured. One can only measure the apparent reflexion angle θ' given by one-half the change in direction of the reflected ray after emergence relative to that of the incident ray before entrance. If the Bragg relation is *incorrectly* applied, using the wave-length *in vacuo* and the apparent reflexion angle θ', an apparent crystal spacing d_n' will be obtained, but it will vary with the order n. The true spacing d can be obtained with sufficient accuracy from any of the values of d_n' by means of the expression $d = d_n'\left(1 + \frac{5{\cdot}4\rho d^2}{n^2} \times 10^{10}\right)$, where d is given in cm. The correction is of the order of $5{\cdot}4 \times 3{\cdot}5 \times 3{\cdot}56^2 \times 10^{-4}\,\% = 0{\cdot}0024\,\%$ in the case of the diamond lattice constant. In using the divergent-beam method of spacing measurement by the method of coincidences, however, the correction is simpler, for a coincidence or near coincidence of rays outside the crystal *must* correspond to a similar coincidence, exact or near, inside the crystal, and all that is necessary, therefore, to obtain the corrected value of a from figure 17 is to use the wave-length λ ($1537{\cdot}416X$) and not λ_0 ($1537{\cdot}400X$) in the formulae used in the construction of the graphs.

Another very necessary correction is that for temperature, because although the expansion of diamond at room temperatures is very small ($3{\cdot}4 \times 10^{-6}$ A/° C; Fizeau 1869), yet since the temperature of the diamonds was about 24° C during the experiments, this does involve a change of $2 \times 10^{-2}X$ if the lattice constant at 18° C is required. Part of the width of the lines may well have been due to a small gradient of temperature, although it could not have been much or it would have shown up more in the high orders. The method could, of course, be modified for use in measuring coefficients of expansion.

Although, as previously mentioned, the half-width at half-maximum of the 313 Cu $K\alpha_1$ line is 0·25 of the α_1-α_2 separation, yet this does not lead to any corresponding uncertainty as to the position of the line maximum, for the lines are reasonably sharp and symmetrical and the maximum can easily be found by eye. The method used for locating the intersections of the lines was to mark on the printed enlargement, with fine pencil lines, the position of maximum intensity of the 313, 133 Cu $K\alpha_1$, 220 Cu $K\alpha_1$ and α_2 absorption lines. The error in a involved in this procedure is certainly not more than 1·5 in 100,000 (corresponding to $\pm 0{\cdot}3$ mm. error in placing Q'' relative to Q) for any one diamond. The values found for four different diamonds varied among themselves by considerably more than this amount. Corrected for refractive index and temperature (to 18° C) the values were:

(1) **3560·00 (± 0·05) *X*** for C 3 T, a diamond cut in the form of a square plate of about 1 mm. thickness, with faces nearly parallel to cube planes, and then treated (by a secret industrial process) in such a way as to turn it black. On prolonged exposure, a Laue photograph of this diamond showed faint graphite lines, but no sign of extra spots except the usual thermal reflexions. It gave excellent divergent-beam photographs (plate 16, figure 21 *a*; plate 17, figure 22 *d*) over a wide range of exposures (3 to 20 sec. at 6 cm.). This diamond was one of several kindly given to me by Messrs Cardimond, Ltd.

(2) **3559·84 (± 0·05) *X*** for GS 1, an octahedral plate of thickness about 2 mm. which had a natural green skin. The diamond as a whole gave faint type I extra spots, but the skin

may possibly have been different in texture from the main body of the crystal. The absorption and reflexion lines were single and very sharp, even in high orders (plate 17, figure 22*a*) giving no indication of any difference in *spacing* between the green skin and the rest of the diamond. This specimen was kindly lent to me by Professor W. T. Gordon, together with several very perfect diamonds of gem quality and some of the specimens used by Robertson, Fox & Martin (1934) in their investigation of the two types of diamond.

(3) **3559·58 (± 0·05) *X*** for 2II, a rounded octahedral plate of thickness about 1 mm., selected from a collection of over 500 industrial diamonds kindly lent to me by the Diamond Trading Company. This was the only diamond in that particular collection that was transparent in the ultra-violet beyond 3000λ. It gave no extra spots on Laue photographs except the usual thermal spots, and also gave excellent divergent beam photographs.

(4) **3559·42 (± 0·10) *X*** for C3U, an untreated, clear octahedral plate also given to me by Messrs Cardimond Ltd., which was a type I diamond, opaque beyond 3000λ, giving strong extra spots on Laue photographs (Lonsdale 1945) and a very poor divergent beam photograph (plate 16, figure 21*b*). The exposure time was critical, and the absorption lines difficult to see, although the resolution was good. It was very noticeable, however, that for this diamond the 313, 133 intersection lay *between* the 220 Cu $K\alpha_1$ and α_2 lines, whereas for the C3T diamond it lay well outside them.

The above values may be compared with that of 3559·48($\pm$0·10) *X* found by a different, but also very accurate method by Renninger (1937), for a clear and obviously perfect diamond of the best gem quality. The divergent beam method cannot be used for such perfect specimens, since they give no absorption pattern at all.

By means of the powder method, which has the advantage of universal applicability, but the disadvantage of giving only a mean value, Riley (1944) found the value 3559·7($\pm$0·1) *X* for a specimen of commercial diamond dust.

The values obtained by Yuching Tu (1932) for two individual diamonds, and by Ehrenberg (1926), also fall within the range found by me for specimens (1)–(4). Using the conversion factor $1000X = 1{\cdot}00203 \pm 0{\cdot}00002$ A,* the values referred to above may be tabulated as shown in table 6 (all at 18° C).

TABLE 6

description of specimen	*a* in *X*	*a* in A	C—C in *X*	C—C in A
C3T, type II (partly graphitized)	3560·00 ± 0·05	3·56723	1541·53 ± 0·02	1·54465
GS1, type I (green skin)	3559·84 ± 0·05	3·56707	1541·46 ± 0·02	1·54458
2II, type II	3559·58 ± 0·05	3·56681	1541·35 ± 0·02	1·54447
C3U, type I	3559·42 ± 0·10	3·56665	1541·27 ± 0·04	1·54440
Tu's diamond 1	3559·72 ± 0·05	3·56695	1541·40 ± 0·02	1·54453
Tu's diamond 2	3559·62 ± 0·05	3·56685	1541·36 ± 0·02	1·54449
Renninger's diamond	3559·48 ± 0·10	3·56671	1541·30 ± 0·04	1·54443
Riley's diamond powder	3559·7 ± 0·1	3·5669	1541·4 ± 0·1	1·5445
Ehrenberg's diamond	3559·7 ± 1·0	3·5669	1541·4 ± 0·4	1·5445

* The *X* unit, used by Siegbahn (1931) for the measurement of X-ray wave-lengths, is about 0·2 % less than 10^{-11} cm. The *X* unit was originally used also in crystal analysis, and in terms of it the effective 200 spacing of NaCl is 2814·00*X* (that is, the apparent spacing uncorrected for refractive index) and the effective first order of the calcite cleavage plane is 3029·04*X*, the real spacing being 3029·45*X*. The exact value of the conversion factor from Siegbahn to metrical units of length is still under discussion, but it will not differ greatly from that given above.

It may therefore be stated that the carbon-carbon distance in diamond is **1541·39** *X* or **1·54451 A**, with a variation of up to **± 0·14 *X* (0·00014 A)** in different diamonds. These variations are almost certainly the result of varying impurity content. The simple method of lattice constant determination described above would not be applicable to most crystals, especially those containing only atoms of low atomic number, because it depends on the existence of *accidental* relationships between high-order (and therefore very much curved) absorption lines. When such high-order lines exist, however, it is always possible, by movement of the crystal or of the film, to produce these relationships intentionally. This method, which involves the use of precision apparatus, was that adopted by Kossel (1936*b*) and van Bergen (1937, 1938, 1941) in their 'Precision measurement of lattice constants by the compensation method', and it obviously has a very wide range of application, the limit of the accuracy of the measurements being set only by the natural breadth of the X-ray emission lines.

Wave-length measurement

Divergent-beam photographs of diamond have also been used to give a precision measurement of the Zn $K\alpha_1$ wave-length (in terms of Cu $K\alpha_1$), again without the use of any kind of precision apparatus. This was done by using a target of brass instead of copper and thus obtaining the zinc and copper lines together on the same film. The use of Zn radiation enables us to record a very high-angle reflexion, that from the (224) plane (plate 17, figure 23 *c*, *d*), and the circles thus obtained intersect a number of other Zn and Cu lines. In general, the greater the number of wave-lengths employed simultaneously, the greater is the chance of finding suitable line intersections from which comparisons of wave-length may be made. The essential point is that the intersections should be those of high-angle (that is, very much curved) lines cutting each other at a small angle. Although the geometry is more complicated when the intersections are *not* symmetrical, it is not difficult, and in theory the method should be capable of high accuracy. In practice, an accuracy of only 1 in 35,000 has been obtained for Zn $K\alpha_1$. This is because the poor conductivity of brass results in a high temperature in the neighbourhood of the point source of X-rays. The diamond, which has to be placed close to the source, itself becomes heated locally, and the resulting temperature gradient in the diamond causes a widening of the absorption lines and a consequent deterioration of resolution. This difficulty could probably be overcome by a deliberate cooling of the diamond in the neighbourhood of the hot source, but since the object of the present paper is rather to illustrate the high accuracy of the results obtained by the simple method used than to push that accuracy to its farthest limit, only the preliminary results are here given.

In figure 18, the intersections of the 224 Zn $K\alpha_1$ and α_2 lines with the 313 Zn $K\alpha_1$ and α_2 and the 220 Cu $K\alpha_1$ and α_2 lines are shown (cf. plate 17, figure 23 *d*, which, of course, shows other lines also in this neighbourhood). These are all parts of circles on the sphere surrounding the X-ray source and distances will be given as angles subtended at the centre. If O is the centre of the 004 circle, A of the 313 circle, B of the 224 circle and C of the 220 circle, all for any wave-length, then in the spherical triangle OAC (figure 19)

$$OA = \tan^{-1}\frac{\sqrt{10}}{3}, \quad OC = 90°, \quad \angle AOC = 45° - \tan^{-1}\frac{1}{3}$$

Hence

$$AC = \cos^{-1} 2\sqrt{\frac{2}{19}}, \quad \angle ACO = \cos^{-1}\frac{3}{\sqrt{11}} = \sin^{-1}\sqrt{\frac{2}{11}}.$$

Let X be the intersection of the 313 and 224 Zn $K\alpha_1$ circles. Then in the spherical triangle AXC,

$$AX = \cos^{-1}\frac{\sqrt{19}}{2}\frac{\lambda_{zn}}{a}, \quad AC = \cos^{-1} 2\sqrt{\frac{2}{19}},$$

and hence

$$\angle ACX = \cos^{-1}\left\{\left[\frac{\sqrt{19}}{2}\frac{\lambda_{zn}}{a} - 2\sqrt{\frac{2}{19}}\cos CX\right]\Big/\sqrt{\frac{11}{19}}\sin CX\right\}$$

$$= \cos^{-1}\{[19\lambda_{zn} - 4\sqrt{2}\,a\cos CX]/2\sqrt{11}\,a\sin CX\}.$$

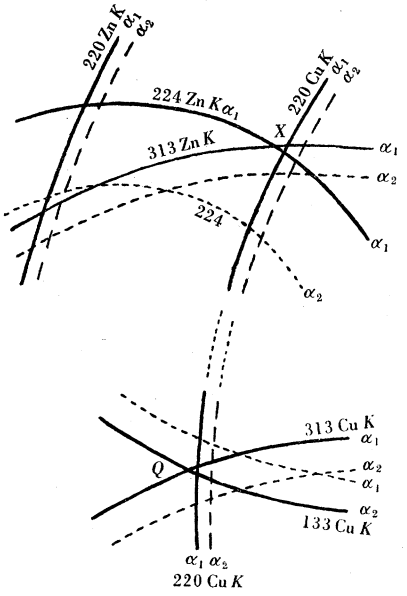

FIGURE 18. Near coincidences of lines found on Cu-Zn photographs of diamond.

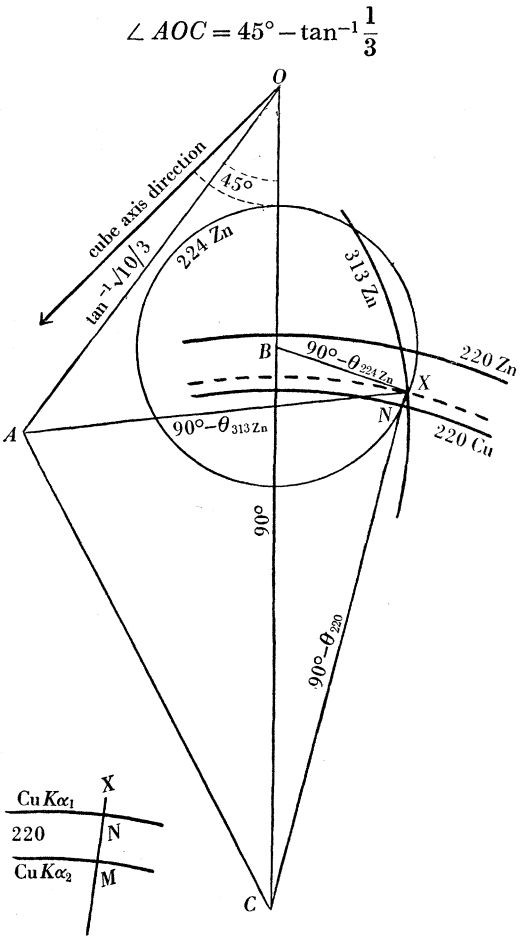

FIGURE 19. Construction from which Zn $K\alpha_1$ wave-length may be calculated in terms of Cu $K\alpha_1$.

In the spherical triangle BCX,

$$BX = \cos^{-1}\sqrt{6}\frac{\lambda_{zn}}{a}, \quad BC = 90° - \tan^{-1}\frac{1}{\sqrt{2}},$$

hence

$$\angle BCX = \cos^{-1}\left\{\left[\sqrt{6}\frac{\lambda_{zn}}{a} - \frac{1}{\sqrt{3}}\cos CX\right]\Big/\sqrt{\frac{2}{3}}\sin CX\right\}$$

$$= \cos^{-1}\{[3\sqrt{2}\,\lambda_{zn} - a\cos CX]/\sqrt{2}\,a\sin CX\}.$$

But

$$\angle ACO + \angle BCX = \angle ACX,$$

or

$$\cos\angle ACO\cos\angle BCX - \sin\angle ACO\sin\angle BCX = \cos\angle ACX. \qquad \text{(i)}$$

The value of CX is best expressed as a function of λ, where λ is a wave-length near to that of Cu $K\alpha_1$, such that if (figure 19, inset) $CN = \cos^{-1}\sqrt{2}\frac{\lambda_{(\mathrm{Cu}\,K\alpha_1)}}{a}$ and $CM = \cos^{-1}\sqrt{2}\frac{\lambda_{(\mathrm{Cu}\,K\alpha_2)}}{a}$, then $CX = \cos^{-1}\sqrt{2}\frac{\lambda}{a}$. The distances XN, MN being small on the film, relative to the crystal to film distance, they may be taken as proportional to the differences of angles involved. All wave-lengths must be expressed as wave-lengths *in the crystal* (that is, corrected for refractive index) and equation (i) then becomes, after substitution

$$\frac{3}{\sqrt{11}}\frac{3\lambda_{zn}-\lambda}{\sqrt{(a^2-2\lambda^2)}}-\sqrt{\frac{2}{11}}\sqrt{\frac{a^2-2\lambda^2-(3\lambda_{zn}-\lambda)^2}{a^2-2\lambda^2}}=\frac{19\lambda_{zn}-8\lambda}{2\sqrt{[11(a^2-2\lambda^2)]}},$$

which reduces to

$$\lambda_{zn}=\frac{26\lambda+2\sqrt{(146a^2-342\lambda^2)}}{73}. \qquad \text{(ii)}$$

In photographs of the 'near coincidence' taken at 80 cm. crystal to film distance, and enlarged, the 224 Zn $K\alpha_1$-α_2 distance is 41 mm., the 220 Cu $K\alpha_1$-α_2 distance (MN) is 4·4 mm. and the 313, 224 Zn $K\alpha_1$ intersection occurs at a distance from the 220 Cu $K\alpha_1$ line such that $XN = 1{\cdot}5$ mm. The value of a can be obtained, as before, from the intersection Q, using figure 17, and it is found to be $3560{\cdot}36X$ at the mean temperature of the diamond, which, as previously mentioned, was certainly high. Hence

$$CN = \cos^{-1}\sqrt{2}\frac{1537{\cdot}416}{3650{\cdot}36} = 52^\circ\,21'\,41''{\cdot}2, \quad CM = \cos^{-1}\sqrt{2}\frac{1541{\cdot}246}{3560{\cdot}36} = 52^\circ\,15'\,4''{\cdot}6,$$

and by proportional parts $CX = 52^\circ\,23'\,56''{\cdot}4$; from which $\lambda = 1536{\cdot}11_3X$.

From equation (ii) $\lambda_{zn\,K\alpha_1} = 1432{\cdot}22_4X$,

or correcting for refractive index (for Zn K and diamond $\mu = 1-\rho = 1-9{\cdot}1\times10^{-6}$)

$$\lambda_{\mathrm{Zn}\,K\alpha_1}\ \textbf{in vacuo} = \mathbf{1432{\cdot}21\ (\pm 0{\cdot}04)}\ \boldsymbol{X}$$

The limits of experimental error would imply a possible mistake of $\pm 0{\cdot}3$ mm. in the estimate of the position of the 313, 133 Cu $K\alpha_1$ intersection relative to 220 Cu $K\alpha_1$ and α_2, and of the 313, 224 Zn $K\alpha_1$ intersection relative to 220 Cu $K\alpha_1$ and α_2, both mistakes adding up.

The determination of the wave-length of Zn $K\alpha_2$ is not accurately possible by this method, first on account of the weakness and diffuseness of the α_2 lines, which make the position of the 313, 224 Zn $K\alpha_2$ intersection much more difficult to determine, and secondly because the distance $X'N$, which is about 63·4 mm., is much too large compared with $MN = 4{\cdot}4$ mm. for the simple 'coincidence' method to be applicable. This illustrates the limitation of the method in its present simple form.

One point that has not been considered above is whether the wave-lengths of the Cu and Zn K X-radiations from an alloy such as brass will be identical with those from pure metals. There is no theoretical likelihood of a measurable difference, but this point could be checked if the diamond temperature were controlled so that a could be used as a standard from one anticathode to another. It is, in any case, interesting to compare the value found in this

experiment for the Zn $K\alpha_1$ wave-length, 1432·21 ($\pm$0·04) X, with the two previous measurements obtained by more orthodox methods:

1432·218 (Bearden & Shaw 1935), 1432·170 (Edlén 1928).

The above work was carried out in the Davy Faraday Laboratory of the Royal Institution, and I am indebted to the Director and to the Managers for the interest they have shown and the facilities given. Other acknowledgements are made in the text. In the experiments on natural ice I was assisted by Miss Jean Smith, whose services were lent to me by the Director of Rothamsted Experimental Station, with the permission of the Agricultural Research Council.

References

Armstrong, A. H. 1929 *Phys. Rev.* **34**, 1115.
Bearden, J. A. & Shaw, C. H. 1935 *Phys. Rev.* **48**, 18.
Bergen, H. van 1937 *Naturwissenschaften*, **25**, 415.
Bergen, H. van 1938 *Ann. Phys., Lpz.*, **33**, 737.
Bergen, H. van 1941 *Ann. Phys., Lpz.*, **39**, 553.
Borrmann, G. 1935 *Naturwissenschaften*, **23**, 591.
Borrmann, G. 1936 *Ann. Phys., Lpz.*, **27**, 669.
Bragg, W. H. 1914 *Nature*, **43**, 31.
Bragg, W. L., Darwin, C. G. & James, R. W. 1926 *Phil. Mag.* **1**, 897.
Bragg, W. L., James, R. W. & Bosanquet, C. H. 1921 *a* *Phil. Mag.* **41**, 309.
Bragg, W. L., James, R. W. & Bosanquet, C. H. 1921 *b* *Phil. Mag.* **42**, 1.
Brill, R., Grimm, H. G., Hermann, C. & Peters, C. 1939 *Ann. Phys., Lpz.*, **34**, 400.
Compton, A. H. & Allison, S. K. 1935 *X-rays in theory and experiment.* London: Macmillan and Co.
Darwin, C. G. 1914 *Phil. Mag.* **27**, 675.
Darwin, C. G. 1922 *Phil. Mag.* **43**, 800.
Edlén, B. 1928 *Z. Phys.* **52**, 364.
Ehrenberg, W. 1926 *Z. Kristallogr.* **63**, 320.
Ewald, P. P. 1918 *Ann. Phys., Lpz.*, **54**, 519.
Ewald, P. P. & Renninger, M. 1934 *The solid state of matter*, **2**, 57. London: Int. Conf. on Phys.
Fizeau, H. 1869 *C.R. Acad. Sci., Paris*, **68**, 1125; *Ann. Phys., Lpz.*, **138**, 26.
Fujiwara, T. 1937 *J. Sci. Hiroshima Univ.* A, **7**, 179.
Fujiwara, T. 1939 *J. Sci. Hiroshima Univ.* A, **9**, 233.
Fujiwara, T. & Onoyama, D. 1939 *J. Sci. Hiroshima Univ.* A, **9**, 115.
Gerlach, W. 1921 *a* *Phys. Z.* **22**, 557.
Gerlach, W. 1921 *b* *Verh. phys. med. Ges. Würzburg*, **56**, 55.
Guinier, A. 1942 *C.R. Acad. Sci., Paris*, **215**, 114.
Hess, B. 1937 *Z. Kristallogr.* **97**, 197. (Gives also reference to unpublished work of F. W. Spiers.)
Hess, B. 1942 *Z. Kristallogr.* **104**, 294.
James, R. W. 1934 *Z. Kristallogr.* **89**, 295.
James, R. W. & Firth, E. M. 1927 *Proc. Roy. Soc.* A, **117**, 62.
Kikuchi, S. 1928 *a* *Proc. Imp. Acad. Japan*, **4**, 354.
Kikuchi, S. 1928 *b* *Jap. J. Phys.* **5**, 83.

PHILOSOPHICAL TRANSACTIONS OF THE ROYAL SOCIETY A MATHEMATICAL, PHYSICAL & ENGINEERING SCIENCES

Kossel, W. 1935 *Gött. Nach. Math. Phys.* **1**, 229.
Kossel, W. 1936*a* *Ann. Phys., Lpz.*, **25**, 512.
Kossel, W. 1936*b* *Ann. Phys., Lpz.*, **26**, 533.
Kossel, W. 1937 *Ergebn. exakt. Naturw.* **16**, 295.
Kossel, W. & Voges, H. 1935 *Ann. Phys., Lpz.*, **23**, 677.
Laue, M. von 1935 *Ann. Phys., Lpz.*, **23**, 705.
Linnik, W. 1929 *Nature*, **124**, 946.
Linnik, W. 1930 *Z. Phys.* **61**, 220.
Lonsdale, K. 1929 *Proc. Roy. Soc.* A, **123**, 494.
Lonsdale, K. 1942*a* *Proc. Roy. Soc.* A, **179**, 315.
Lonsdale, K. 1942*b* *Proc. Phys. Soc. Lond.* **54**, 339.
Lonsdale, K. 1943 *Rep. Progr. Phys.* **9**, 256. London: Physical Society.
Lonsdale, K. 1944 *Nature*, **153**, 433.
Lonsdale, K. 1945 *Nature*, **155**, 572.
Onoyama, D. 1939 *J. Sci. Hiroshima Univ.* A, **9**, 125.
Ponte, M. 1927 *Phil. Mag.* **3**, 195.
Renninger, M. 1934 *Z. Kristallogr.* **89**, 344.
Renninger, M. 1937 *Z. Phys.* **106**, 141.
Riley, D. P. 1944 *Nature*, **15**, 587.
Robertson, R., Fox, J. J. & Martin, A. E. 1934 *Phil. Trans.* A, **232**, 463.
Robinson, B. W. 1933 *Proc. Roy. Soc.* A, **142**, 422.
Robinson, B. W. 1934 *Proc. Roy. Soc.* A, **147**, 467.
Rutherford, E. & Andrade, E. N. da C. 1914 *Phil. Mag.* **28**, 263.
Seemann, H. 1916 *Ann. Phys., Lpz.*, **51**, 391.
Seemann, H. 1917 *Ann. Phys. Lpz.*, **53**, 461.
Seemann, H. 1919 *Phys. Z.* **20**, 169.
Seemann, H. 1930 *Ann. Phys., Lpz.*, **6**, 793; **7**, 633.
Seemann, H. & Kantorowicz, O. 1930 *Naturwissenschaften*, **18**, 526.
Siegbahn, M. 1931 *Spectroskopie der Röntgenstrahlen*, 2nd ed. Berlin: Julius Springer.
Tu, Y. C. 1932 *Phys. Rev.* **40**, 662.
Voges, H. 1936 *Ann. Phys., Lpz.*, **27**, 702.
Wennerlöf, I. 1930 *Ark. Mat. Astr. Fys.* A, **22**, no. 8.

Description of Plates

Plate 16

Figure 20. *a*. Hexamine. 5 sec. exposure in semi-cylindrical camera radius 6 cm. *Before* cooling in liquid air the pattern is almost invisible. *b*. Hexamine. Same: *after* cooling in liquid air the pattern is quite clear, and remains permanently. *c*. Benzophenone: 90 sec. at 15 cm. crystal to film distance. Note the absence of curved lines. *d*. Ice: (0001) nearly parallel to film. (The diffuse circular rings on this and some other photographs are due to unwanted scattering from internal walls of the anticathodes used.)

Figure 21. *a*. Diamond C3T. Type II, giving no 'extra' spots on Laue photographs. Excellent divergent beam patterns over a wide range of exposures; showing coincidence *Q*. *b*. Diamond C3U. Type 1, giving strong 'extra' spots on Laue photographs. Poor divergent beam pattern: time of exposure critical; cf. 21*a*. *c*. Coincidence *A* (cf. figure 12). *d*. Coincidence *Q* (cf. figure 12).

PLATE 17

FIGURE 22. *a*. Diamond GS 1. Every possible reflexion (including high-angle 224 Cu $K\beta$) gives an absorption line of clear visibility. Use of plane film restricts extent of pattern. *b*. Diamond D 19 (Robertson *et al.* 1934) showing marked spreading of lines, but 224 Cu $K\beta$ still relatively sharp and intense in one sector. *c*. Diamond Moppe 7, showing sharpness of reflexion lines, and comparative weakness of all but 111 absorption lines. *d*. Diamond C 3 T. Process film used to sharpen lines; showing how the 331α and α_2 bracket the 111α, line. 224 Cu $K\beta$ lines intersect near upper centre of film.

FIGURE 23. *a*. Diamond C 1 T; cube face parallel to anticathode surface; portion of cylindrical film (axis vertical). To be compared with figures 10 and 12 (Kossel and stereographic projections). *b*. Diamond D 20 (Robertson *et al.* 1934); random orientation, but obviously with (331) plane nearly parallel film; trigonal axis emerging near lower left corner. *c*. Diamond GS 1, brass anticathode, showing Zn $K\alpha_1$, α_2 224 circles, intersecting 220, 111, 331, 113, 004 Cu and Zn lines. 224 plane nearly parallel to film. *d*. Same enlarged, 220 Cu $K\alpha$ and Zn $K\alpha$ lines nearly horizontal, 111 lines sloping vertically. Zn $K\beta$ too weak to be seen, although Cu $K\beta$ lines are quite strong.

PHILOSOPHICAL TRANSACTIONS OF THE ROYAL SOCIETY A MATHEMATICAL, PHYSICAL & ENGINEERING SCIENCES

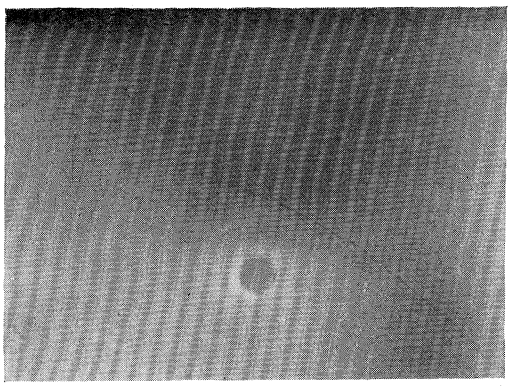

20*a*

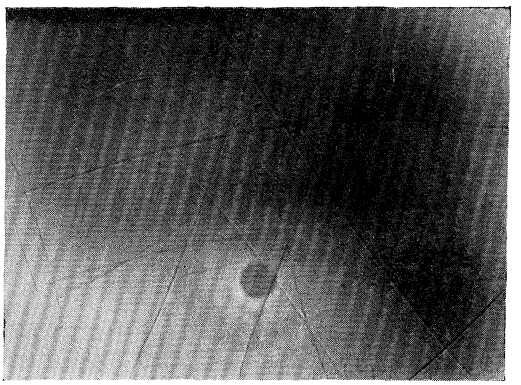

20*b*

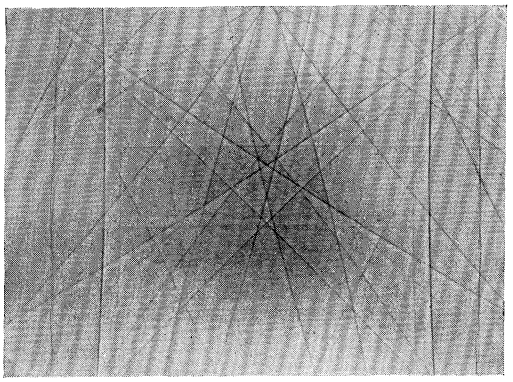

20*c*

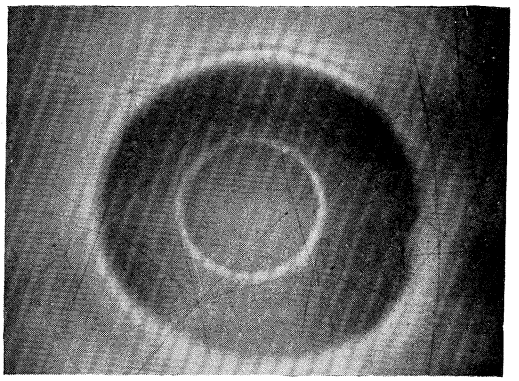

20*d*

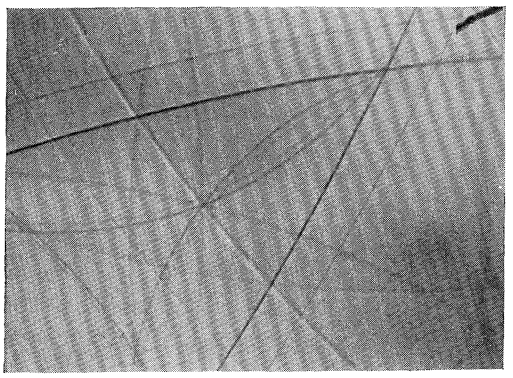

21*a*

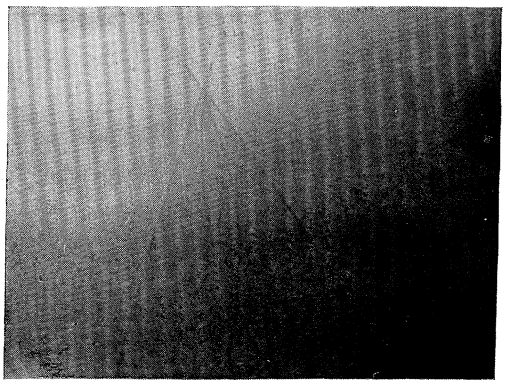

21*b*

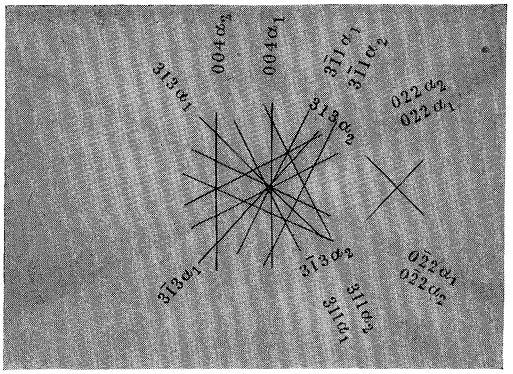

21*c*

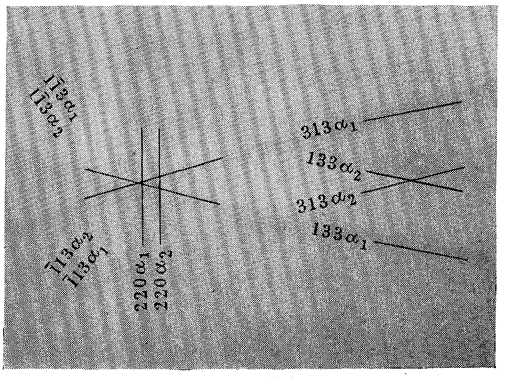

21*d*

(*Facing p.* 250)

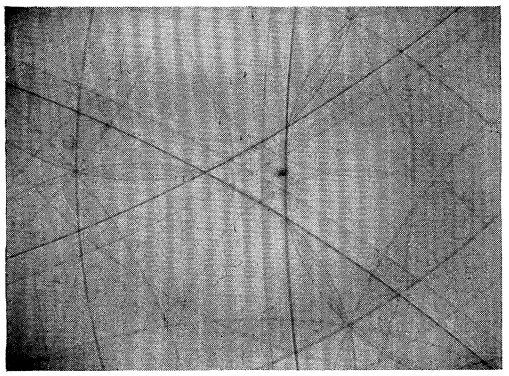

22 *a*

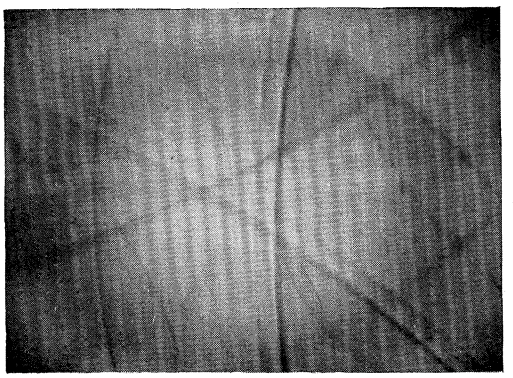

22 *b*

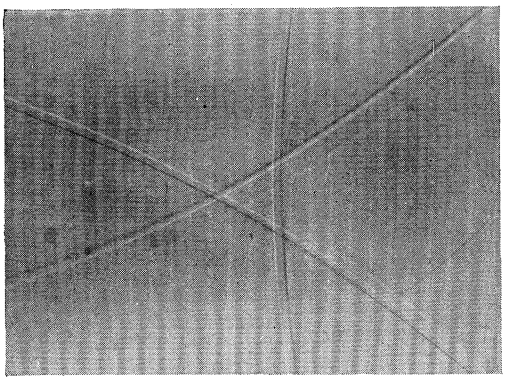

22 *c*

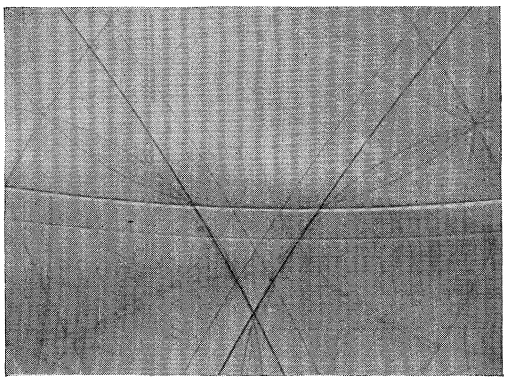

22 *d*

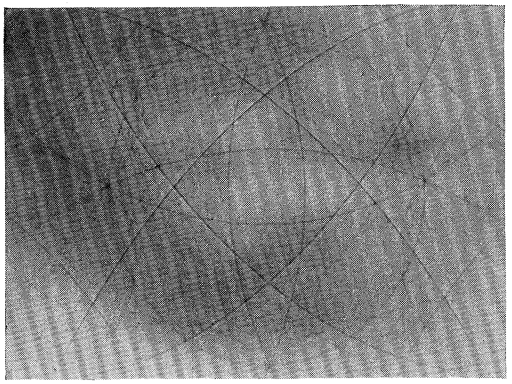

23 *a*

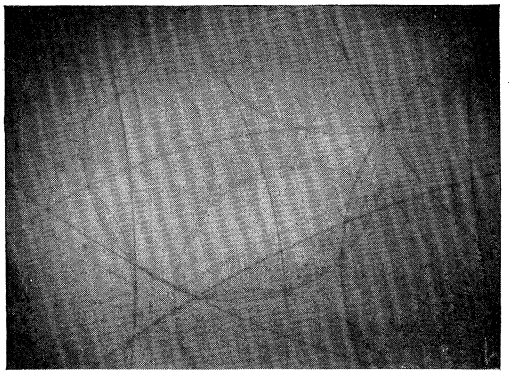

23 *b*

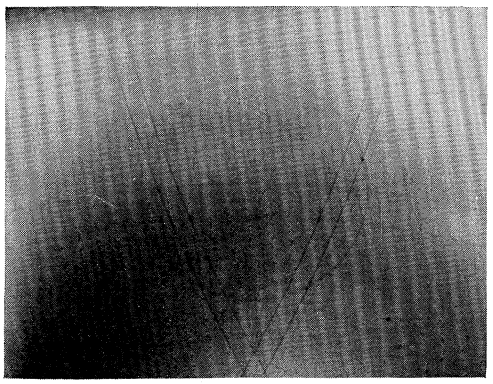

23 *c*

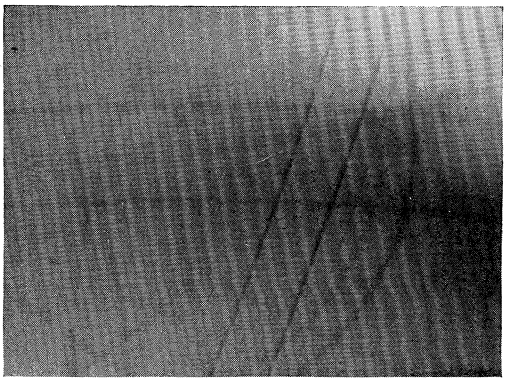

23 *d*

PHILOSOPHICAL TRANSACTIONS OF THE ROYAL SOCIETY A MATHEMATICAL, PHYSICAL & ENGINEERING SCIENCES

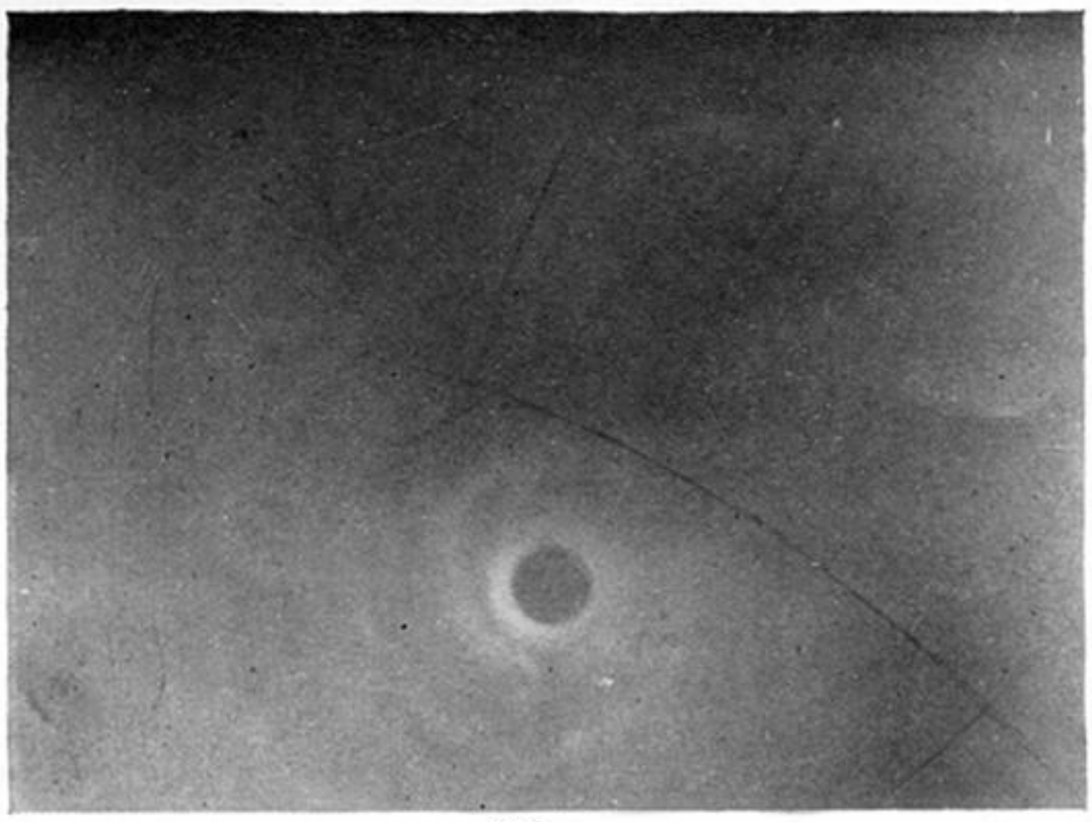

20 *a*

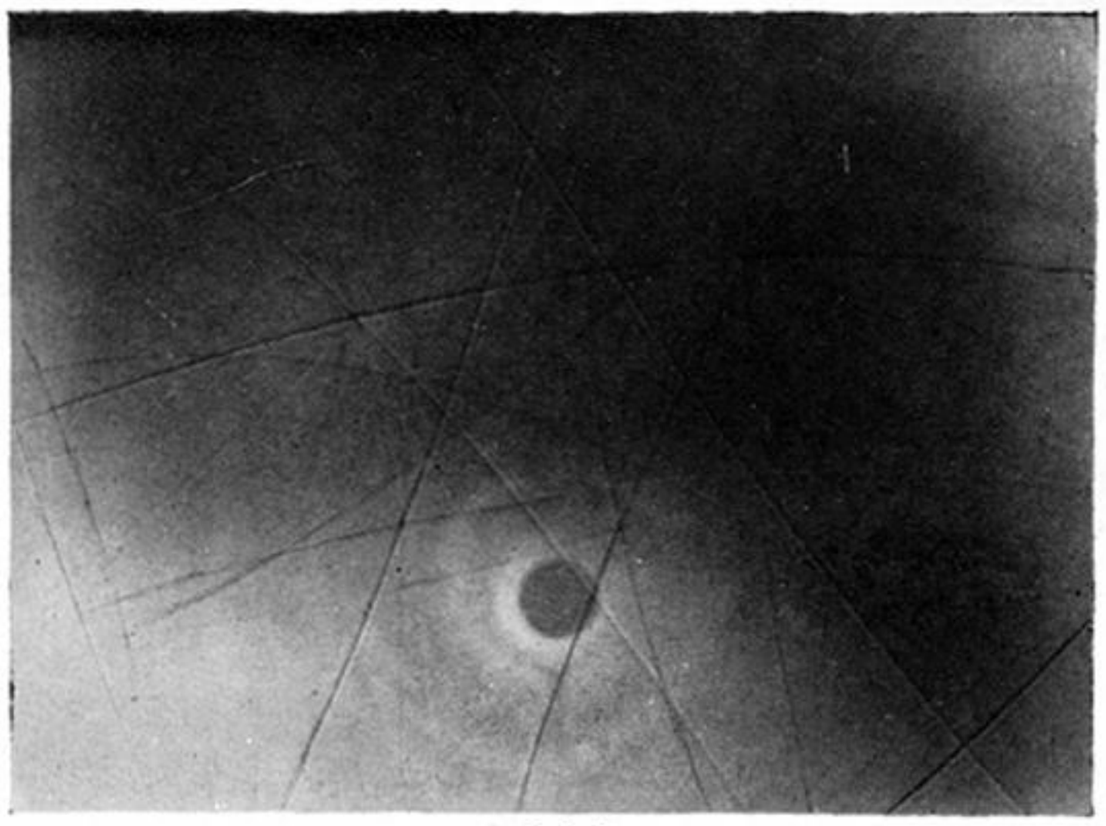

20 *b*

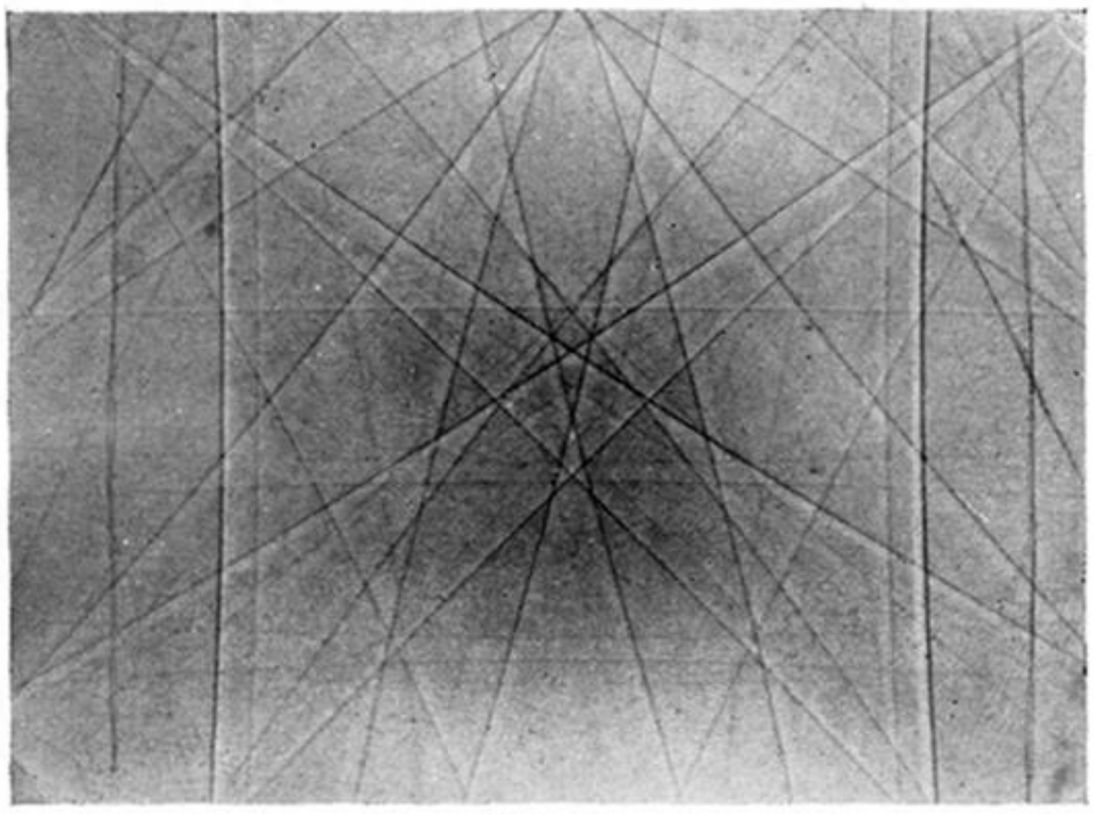

20 *c*

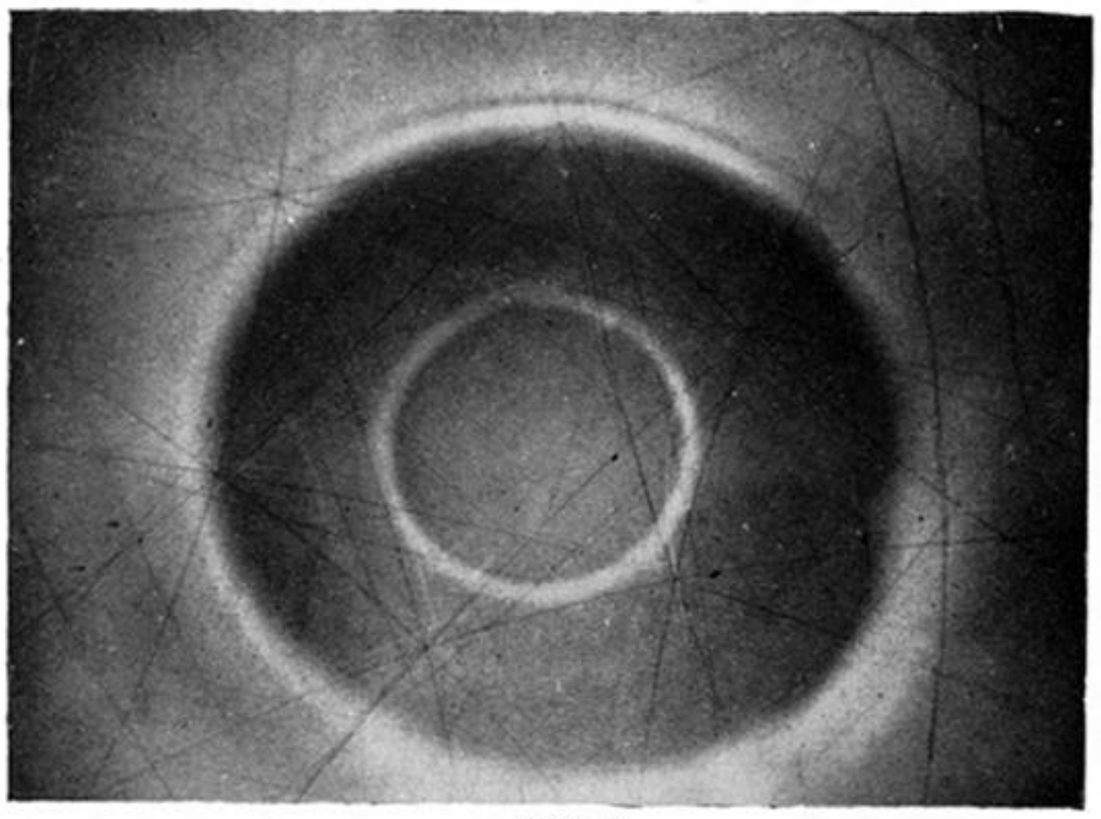

20 *d*

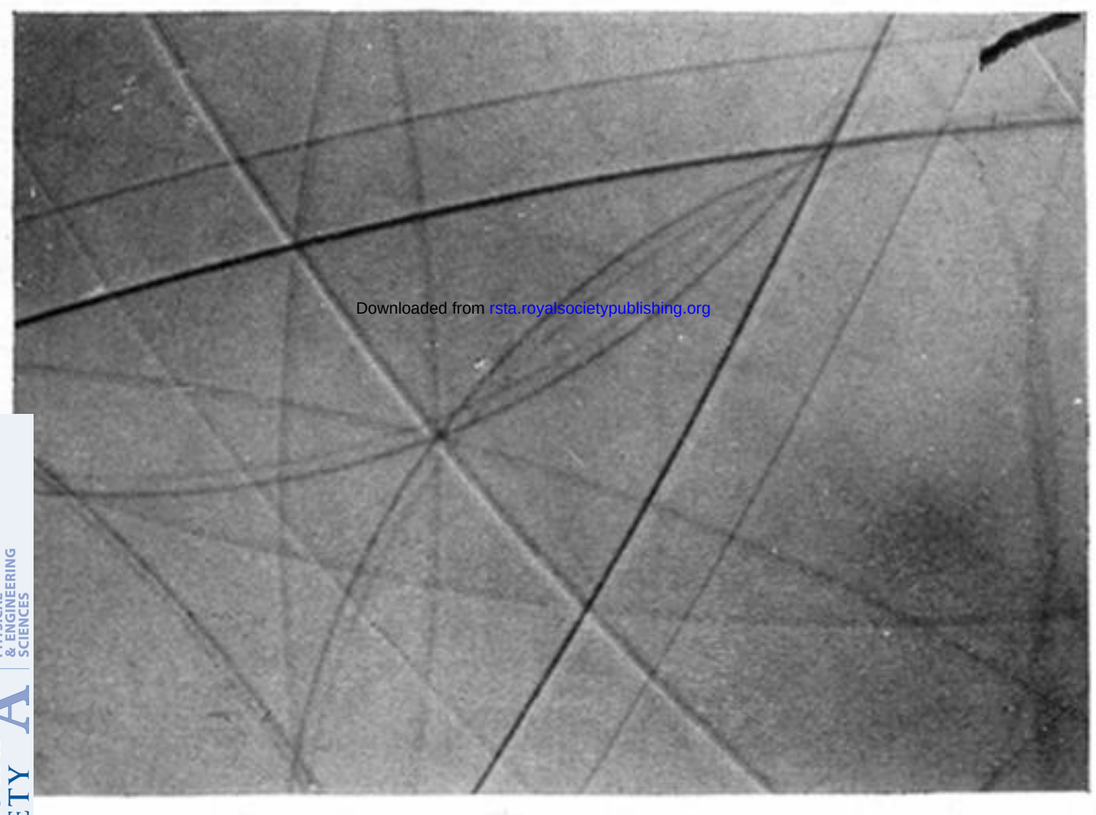

21 *a*

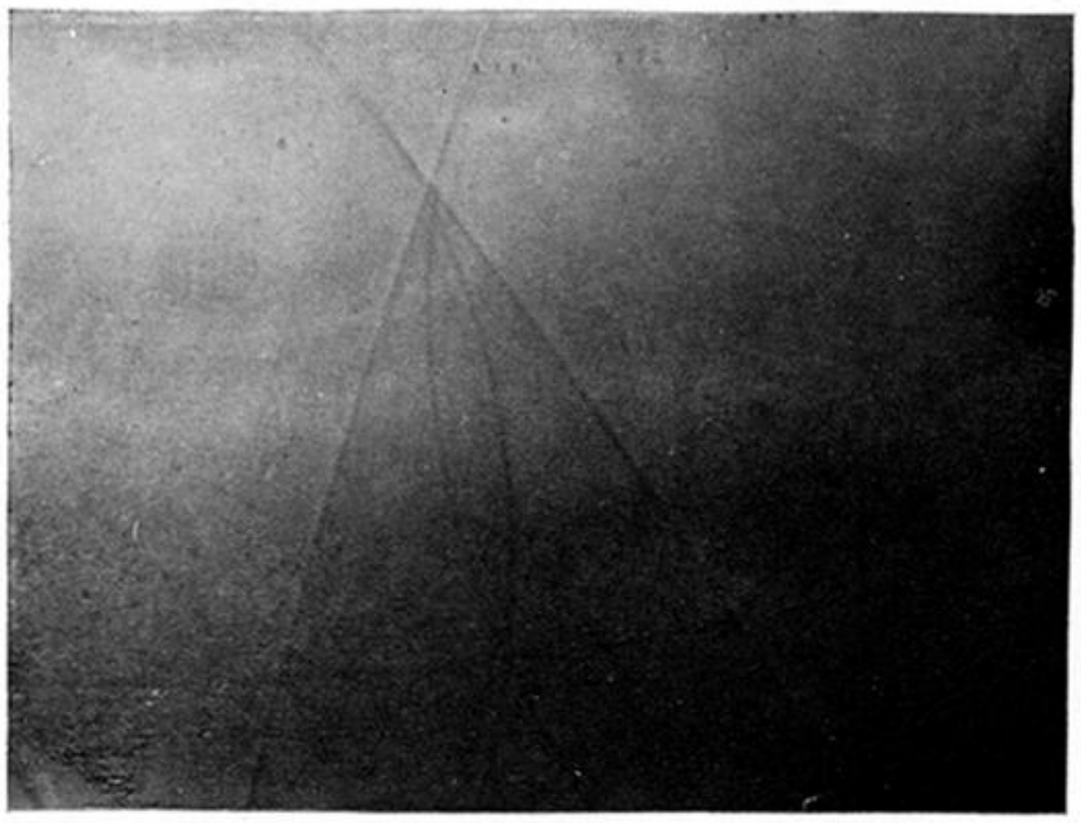

21 *b*

21 *c*

21 *d*

(*Facing p.* 250)

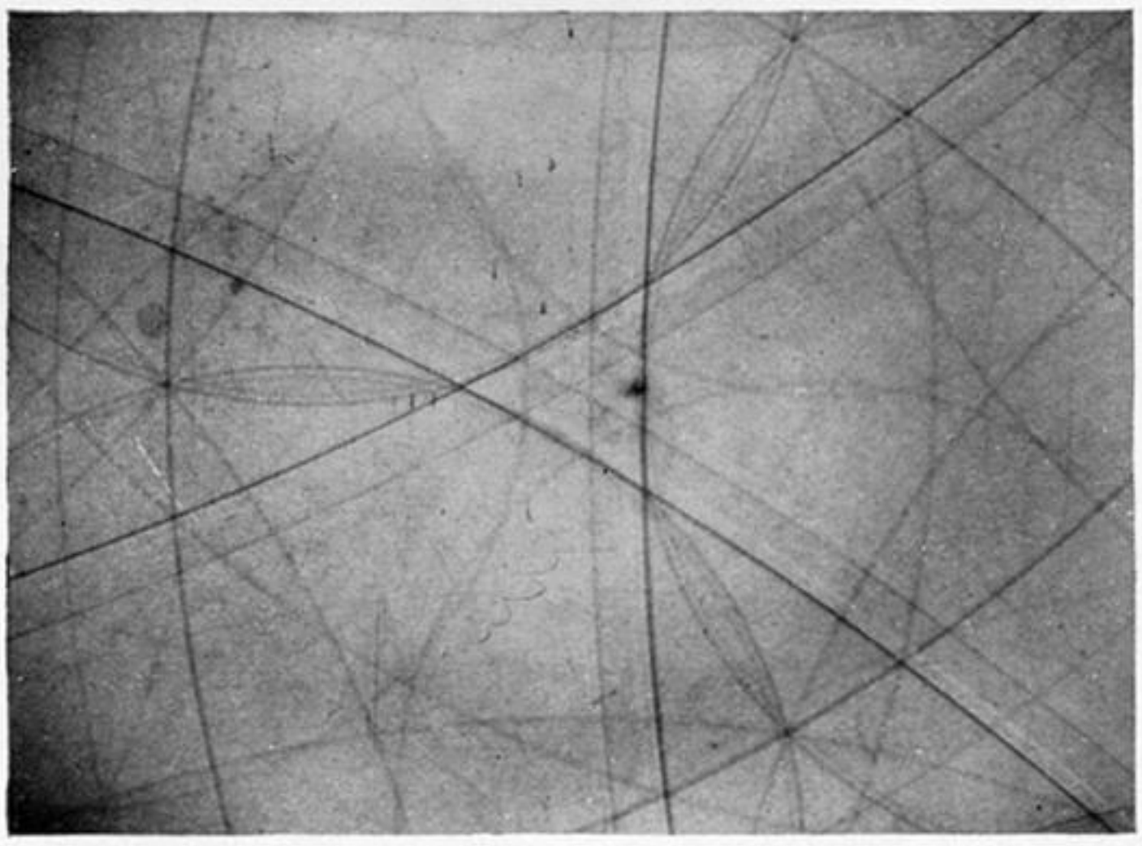

22 *a*

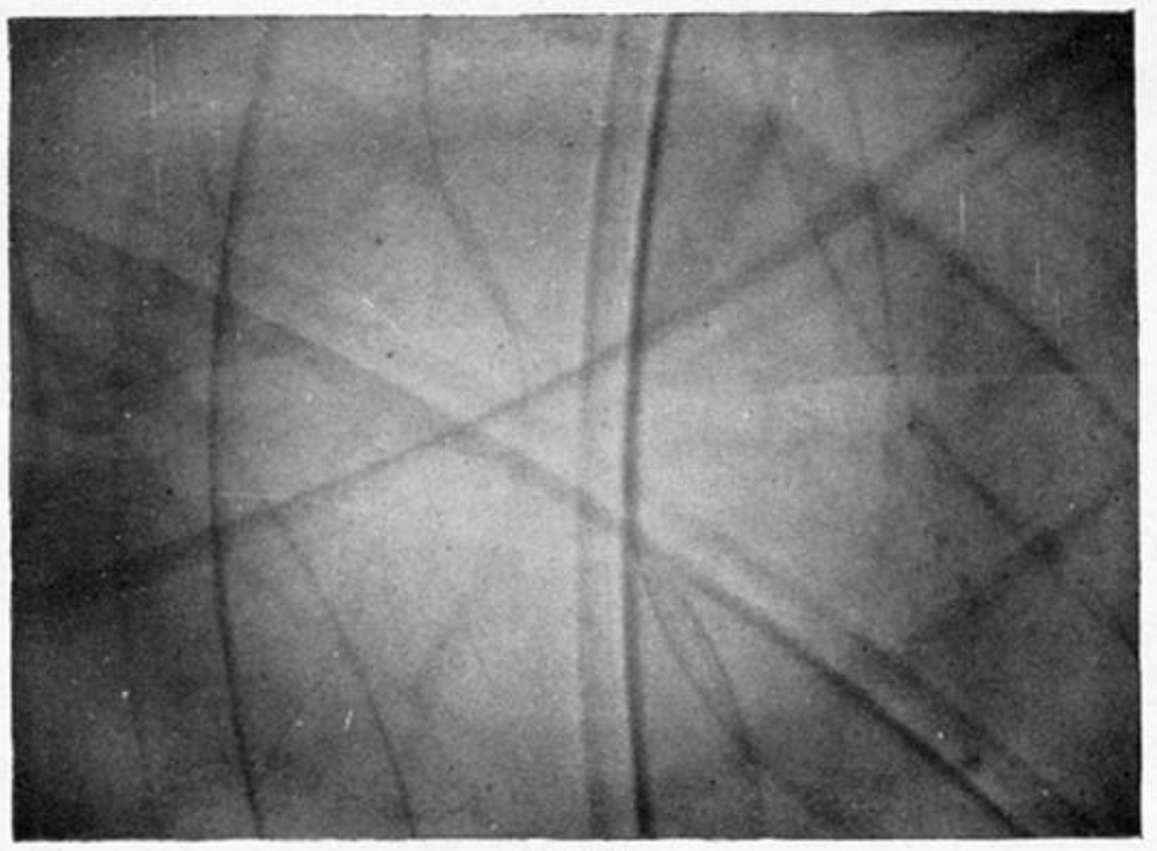

22 *b*

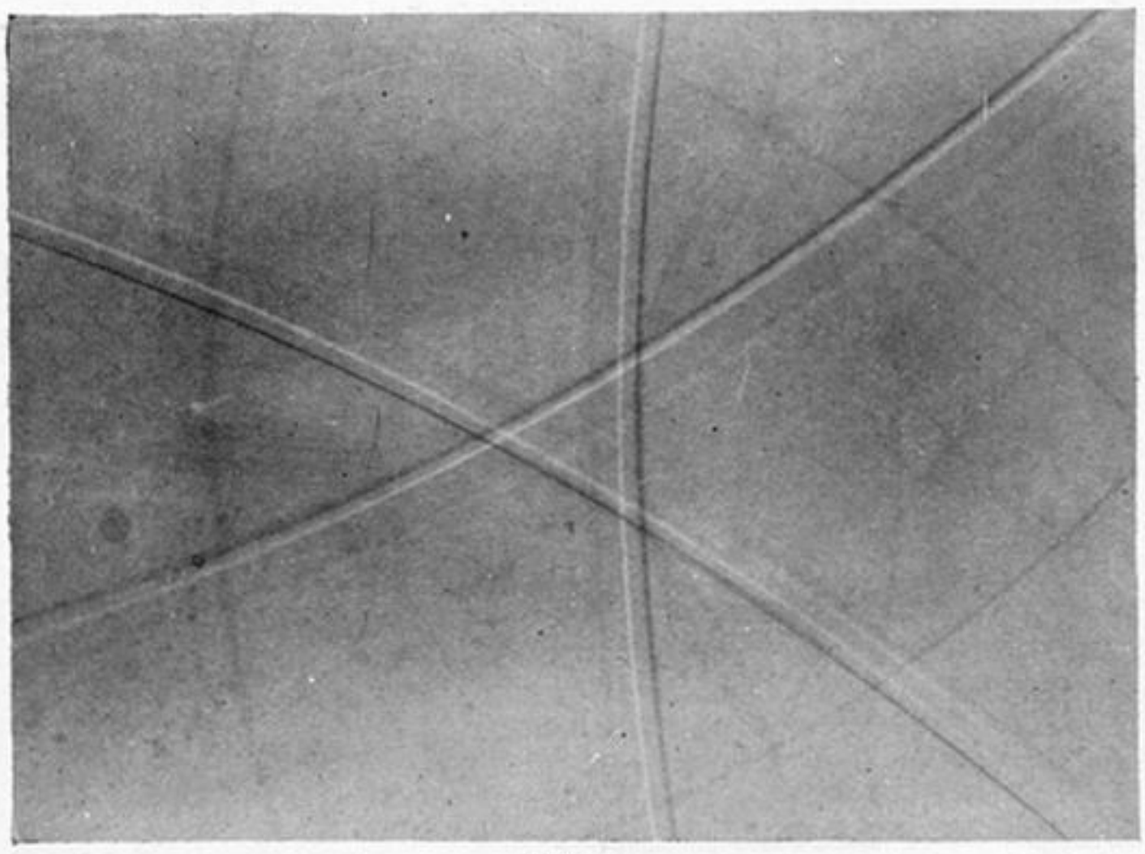

22 *c*

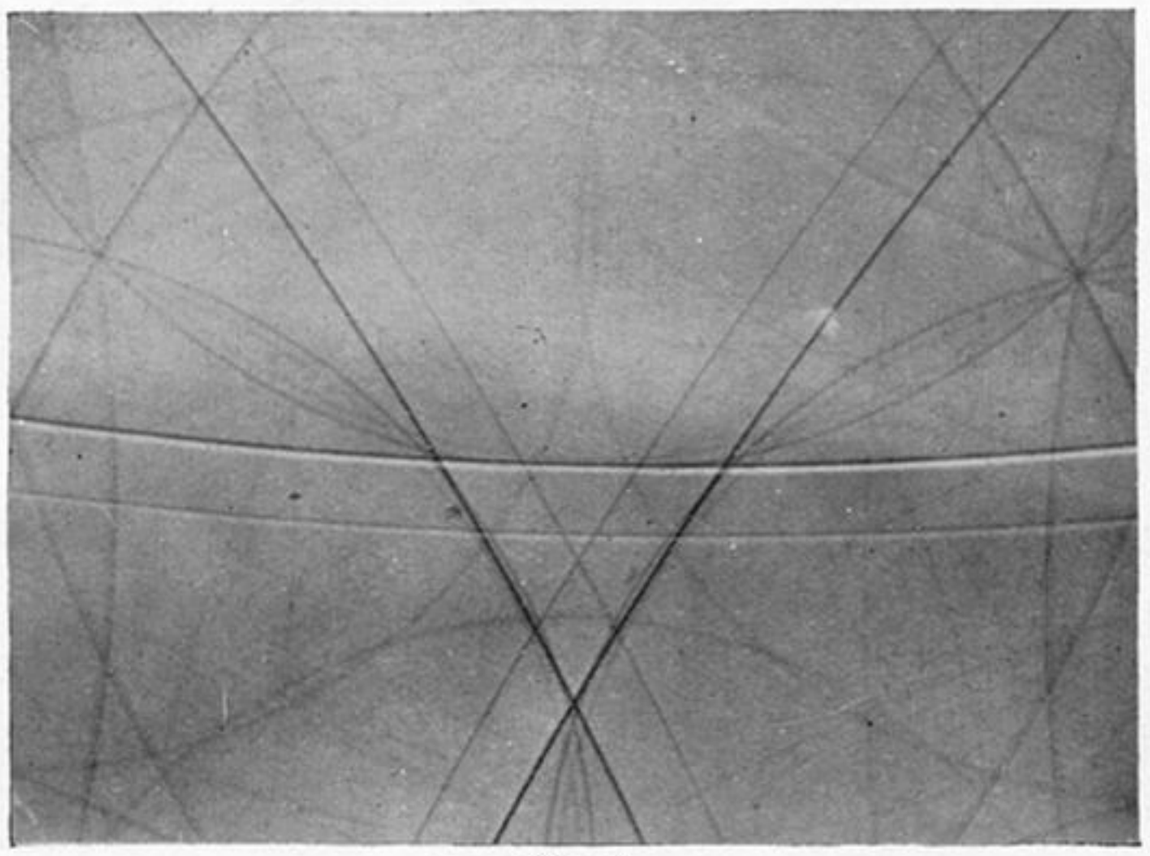

22 *d*

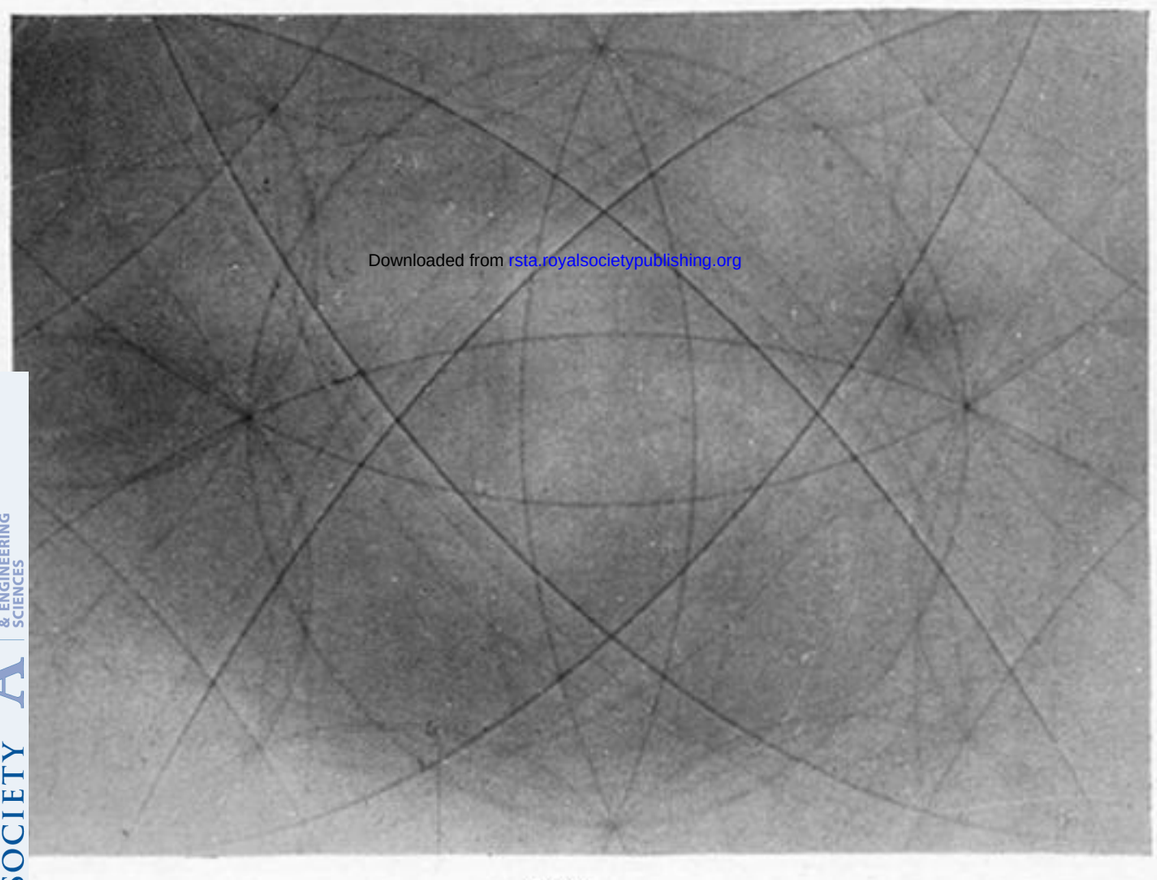

23 *a*

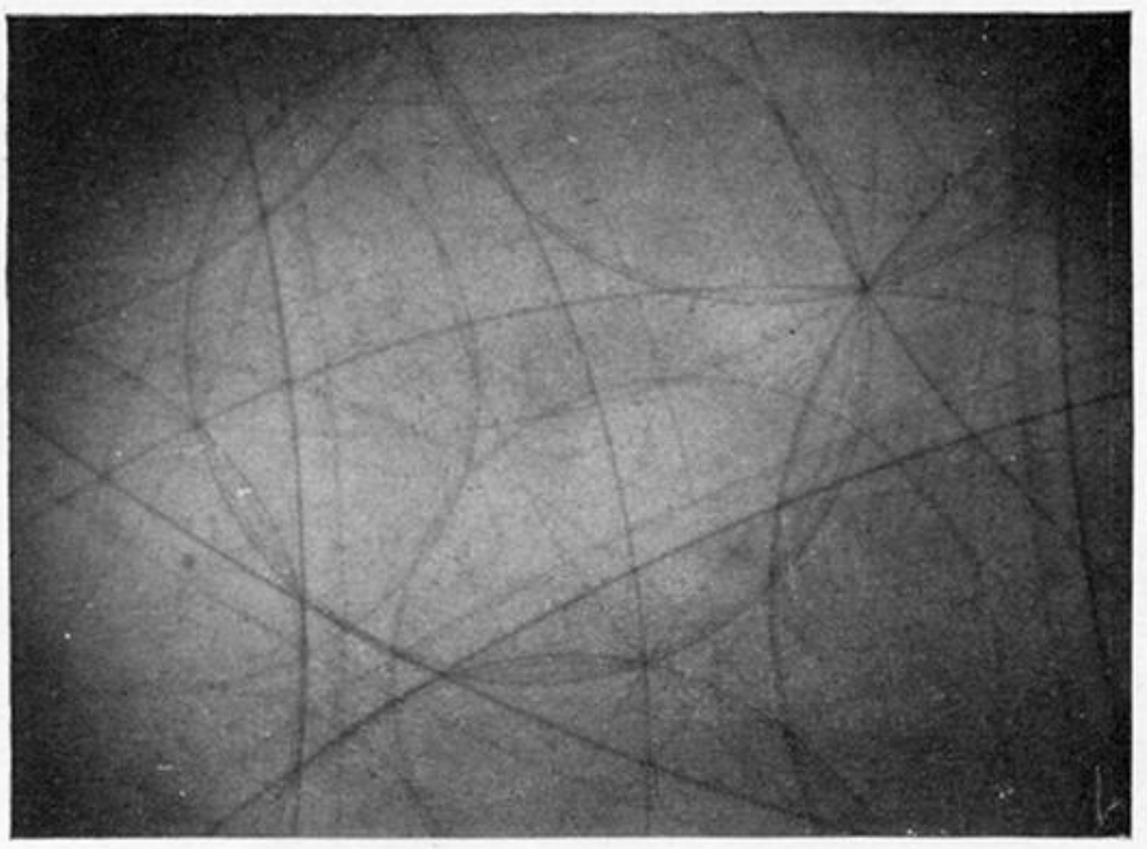

23 *b*

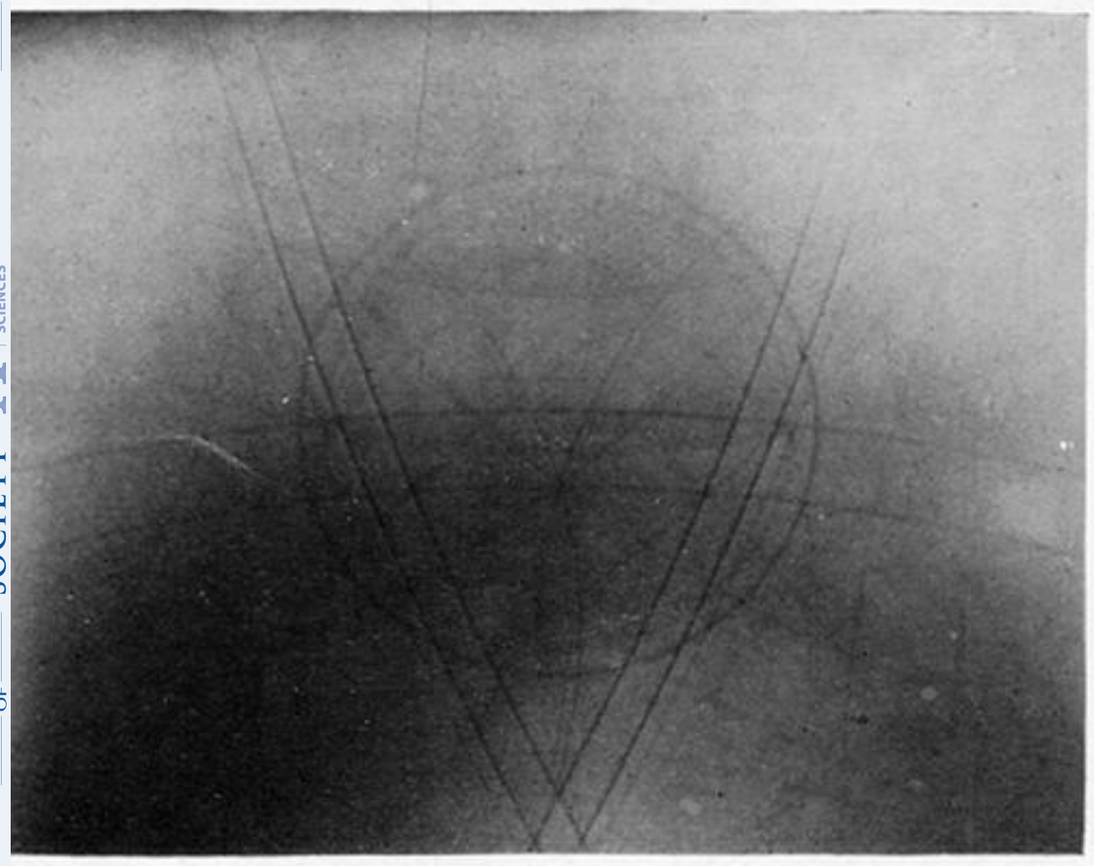

23 *c*

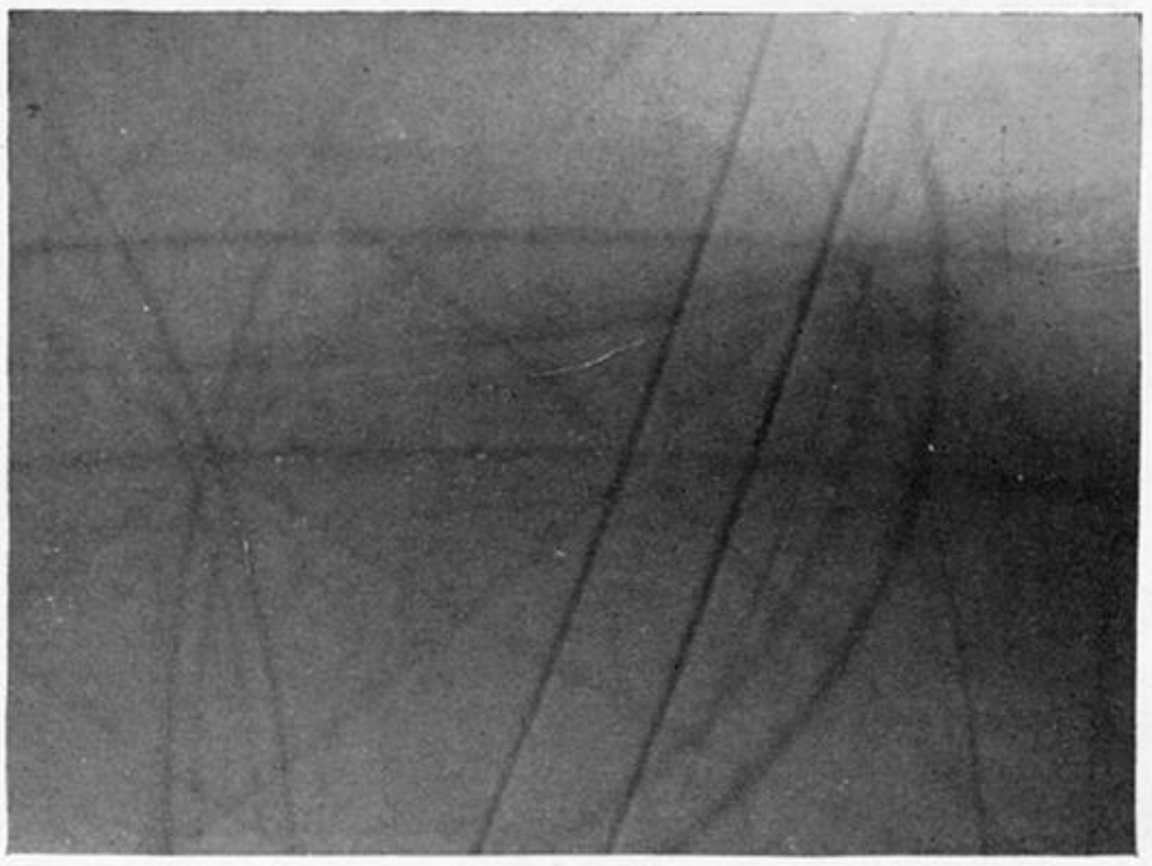

23 *d*